



**HAL**  
open science

# Self-Assembled Artificial Ion-Channels toward Natural Selection of Functions

Shao-ping Zheng, Li-bo Huang, Zhanhu Sun, Mihail Barboiu

► **To cite this version:**

Shao-ping Zheng, Li-bo Huang, Zhanhu Sun, Mihail Barboiu. Self-Assembled Artificial Ion-Channels toward Natural Selection of Functions. *Angewandte Chemie International Edition*, 2021, 60 (2), pp.556-597. 10.1002/anie.201915287 . hal-02962172

**HAL Id: hal-02962172**

**<https://hal.umontpellier.fr/hal-02962172v1>**

Submitted on 1 Nov 2021

**HAL** is a multi-disciplinary open access archive for the deposit and dissemination of scientific research documents, whether they are published or not. The documents may come from teaching and research institutions in France or abroad, or from public or private research centers.

L'archive ouverte pluridisciplinaire **HAL**, est destinée au dépôt et à la diffusion de documents scientifiques de niveau recherche, publiés ou non, émanant des établissements d'enseignement et de recherche français ou étrangers, des laboratoires publics ou privés.

---

# Self-assembled Artificial Ion-Channels toward Natural Selection of Functions

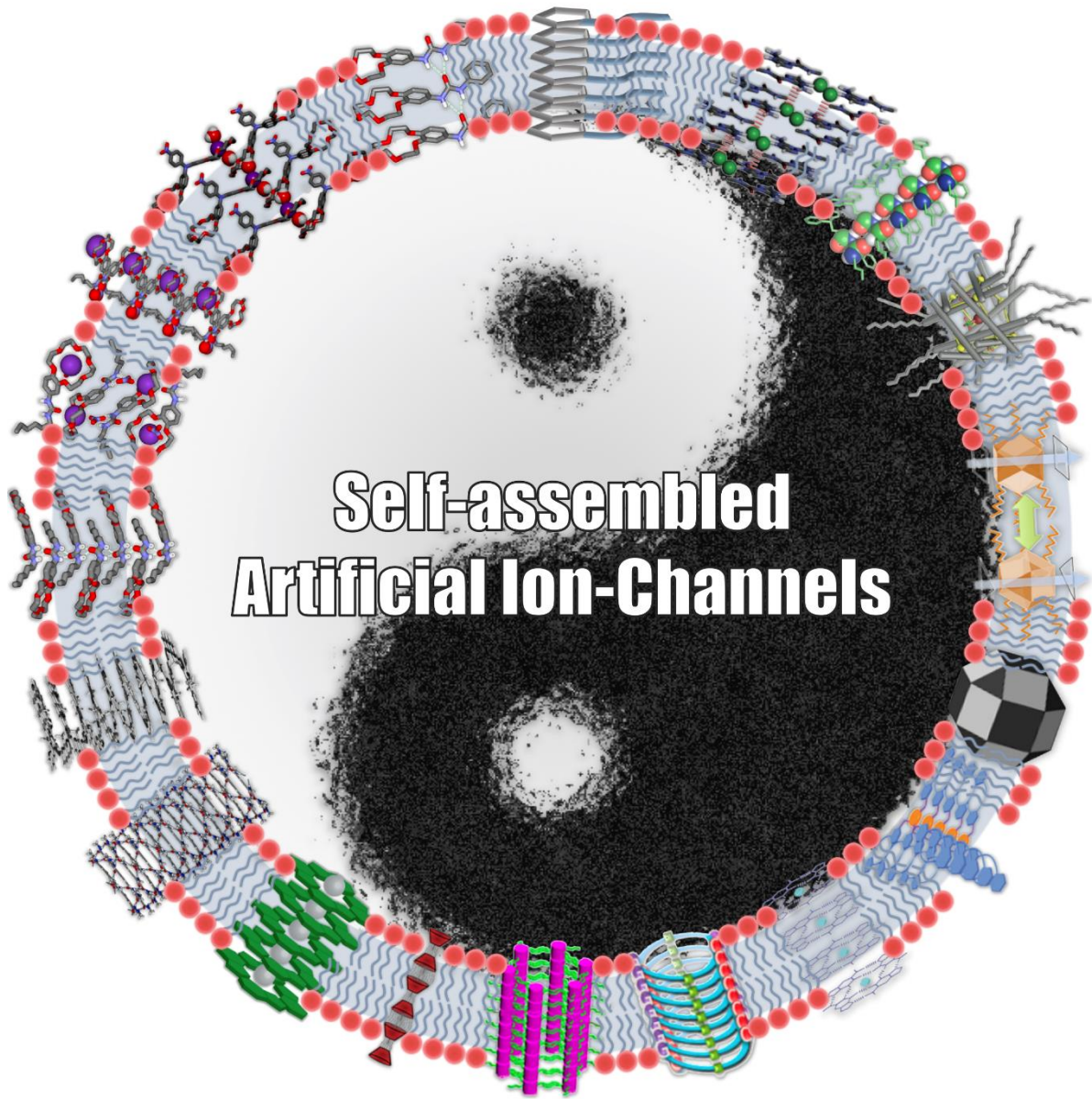
Shao-Ping Zheng,<sup>1,2</sup> Li-Bo Huang<sup>1,2</sup> Zhanhu Sun,<sup>2</sup> Mihail Barboiu,<sup>1,2\*</sup>

1. Lehn Institute of Functional Materials, School of Chemistry, Sun Yat-Sen University, Guangzhou 510275 (China)

2. Institut Européen des Membranes, Adaptive Supramolecular Nanosystems Group, University of Montpellier, ENSCM-CNRS Place E. Bataillon CC047, 34095 Montpellier (France)

**Key words:** Self-assembly, ion-channels, macrocycles, bilayer membranes, biomimetic

**Abstract:** Owing to their significant physiological functions, especially as selective relays for translocation of physiological relevant species through cellular membranes, natural ion channels play important role in the living organisms. During the last decades, the field of self-assembled ion channels has been continuously developed. Convergent multidimensional self-assembly strategies have been used for the synthesis of unimolecular channels or non-covalent self-organized channels, designed to mimic natural ion channel proteins and for which a rich array of interconverting or adaptive channel conductance states can be observed. In this review, we give an overview on the development of various self-assembled artificial channels in a bottom-up approach, especially their design, self-assembly behaviour, transport activity in lipid bilayer membranes, mechanism of transport and comparison with natural ion channels. Finally, we discuss their applications, the potential challenges facing in this field as well as future development and perspectives.





Shao-Ping Zheng received her Bachelor degree in Chemical Engineering and Technology in 2014 from Sun Yat-Sen University, China, where she continued her doctoral study in Chemistry under the supervision of Prof. Mihail Barboiu. Currently she is working in Prof. Mihail Barboiu's group in IEM, France as an exchanging PhD student, focusing on biomimetic supramolecular ion channel design and functionalization.



Li-Bo Huang obtained a BSc in chemistry from Sun Yat-Sen University in 2016, then he stayed on for a PhD in Prof. Cheng-Yong Su's group. He is currently working under the supervision of Prof. Mihail Barboiu towards a joint PhD in chemistry at Institut Européen des Membranes in France. His research interests are artificial water channels and transmembrane cation transport.



Zhanhu Sun obtained M.S. degree (2010) in Prof. Yu Liu's group in Nankai University and PhD degree (2013) in RWTH Aachen University supervised by Prof. Markus Albrecht. Between 2014 to 2017, he co-worked with Prof. Mihail Barboiu in University of Montpellier in France, Prof. Hongchao Guo in China Agricultural University in China and Prof. Zheng-Rong Lu in Case Western Reserve University in US. In 2018, he joined Prof. David Leigh's group in East China Normal University in Shanghai. He is one of the 2013 SciFinder® Future Leaders in Chemistry. His research ranges from supramolecular chemistry, organic synthesis, catalysis to the applications of synthetic products in BME and artificial channels.



Mihail Barboiu is CNRS Research Director at the Institut Européen des Membranes in Montpellier and Fellow of Royal Society of Chemistry. A major focus of his research is Dynamic Constitutional Chemistry toward Dynamic Interactive Systems: biomimetic membranes, delivery devices etc. Author of more than 230 scientific publications, 3 books and 22 chapters and 400 conferences and lectures, Dr. Barboiu has received in 2004 the EURYI Award in Chemistry and in 2015 the RSC Surfaces and Interfaces Award for the development of artificial water channels.

## 1. Introduction

**Natural channels.** Cell membrane, separating the interior intracellular space from the outside extracellular environment is essential for life. Functioning as gatekeepers, semi-permeable phospholipid membranes regulate the exchange of ionic or molecular metabolites. Due to the structural incompatibility of the hydrophilic metabolites and the hydrophobic cell membranes, ions or molecules cannot diffuse through cell membrane and their translocation may be facilitated by ion-channels or carriers. Natural ion channels are pore-forming proteins, regulating the flow of ions from either side of the cell membrane to the other, in response to external stimuli like pH, ionic strength, water content, etc. Their activities involve many physiological processes: cell proliferation and signalling, trans-epithelial transport, signal transduction and their dysfunctions can lead to *-channelopathies-* such as diseases of the nervous system (generalized epilepsy or hemiplegic migraine), of the respiratory system (cystic fibrosis), of the endocrine system (diabetes), of the immune system (Isaac syndrome, anti-NMDA receptor encephalitis) or renal disease (Bartter's syndrome).

**Supramolecular artificial channels.** Parallel to the investigation of natural ion channels intensive research efforts are devoted to create synthetic ion channels using artificial compounds.<sup>[1]</sup> The main strategies are related with the synthesis of unimolecular channels or the design of self-assembled supramolecular channels exploiting aggregation of small molecular components to produce active membrane-spanning structures. They are constructed by employing various non-covalent bonds, such as hydrogen-bonding, electrostatic, metal-coordination, host-guest, ion- $\pi$  interactions or halogen bonding, which are reversible, error correcting, and ready availability. Artificial channels can be used not only in curing

---

channelopathies, but also for the understanding the natural ion channel functions and therefore paving the way for a wide range of applications in water treatment, biosensing, nanotechnologies and drug delivery. Supramolecular artificial channels, as a significant mimic approach to simulate the self-assembly process of natural proteins in lipid bilayer membranes in both structures and functions, have many advantages, such as controllable transport properties, versatility and diversity due to their inherent adaptive properties. These characteristics enable us elucidate and understand the detailed mechanism of transport and structure–function correlation. In this review our focus is to present the status of art for construction of bottom-up artificial ion channels *via* supramolecular self-assembly.

**Design of the supramolecular ion channels.** The basic strategy for the construction of supramolecular ion channels is to self-ensemble simple molecular components through non-covalent interactions and in a controlled manner to generate directional translocating pathways for an ion channel mechanism. Three main factors have to be carefully considered for the construction of molecular components: i) lipophilicity, ii) the overall length of the channel and iii) the ion-recognition sites. Lipophilicity is a significant factor determining the valid insertion of the supramolecular ensemble into a membrane to form an ion channel. The overall length of supramolecular ensemble needs to span the phospholipid bilayer membranes thickness of  $\sim 35$  Å. The introduction of recognition sites for the selective ion binding is the highly important to regulate the selectivity of the transport. Notably, the interactions between ions and the recognition sites can neither be too weak nor too strong. The resulting flux in competitive transport experiments does not show a linear dependency with the ion-receptor stability constant: too strong binding of the solute has a negative effect on the transport selectivity. If the

---

interactions are too weak, good selectivity cannot be achieved; while, too strong, the transport ability will be significantly affected since the transport process involves both loading and release of guests (ions). Therefore, there exists an optimal association constant for obtaining good transport selectivity.

The discussion will be divided into two parts: *supramolecular artificial cation channels* and *supramolecular artificial anion channels*, majorly due to the different driving forces involved.

In biological channels, cation selectivity often originates from the ion coordination, while hydrogen-bonding, ion pairing and anion–dipole interactions contribute to selectivity of anion transport. In this review, we focus on recent breakthroughs and outline the emerging concepts used for the design of supramolecular artificial ion channels, the resultant self-assembled channel structures, the transport mechanisms, the structure-function relationship, and comparison to natural artificial ion channels. Along the manuscript, we will emphasize the strategies of how to detect and describe the selectivity sequences and cooperative multi-ion hopping mechanisms along the self-assembled channels and finally, we will discuss their future development. We selected examples from major players in the field of synthetic ion channels and pores, including our own work.

## 2. Supramolecular artificial cation channels

**Macrocyclic artificial channels.** There is a huge diversity of macrocyclic compounds that have been extensively used to build ion-channels, i.e. crown-ethers,<sup>[1]</sup> cyclodextrins (CDs)<sup>[2]</sup>, cucurbit[n]urils (CBs),<sup>[3]</sup> calix[n]arenes (CAs),<sup>[4]</sup> pillar[n]arenes (PAs)<sup>[5]</sup>.

In this section, we will focus on selected recent examples on crown ether-based artificial

channels. Crown ethers are a class of simple amphipathic molecules. Their oxygen atoms in repeating  $-\text{OCH}_2\text{CH}_2-$  ether units point toward the center of the molecule, making the inner core hydrophilic, while outwardly oriented ethylene moieties confer to the external surface lipophilic properties. Since their inception, a variety of tailored crown-ethers have been successfully used as transporters in liquid membranes which accounts for their ability as ion phase-transfer catalysts. Gokel,<sup>[6]</sup> Fyles<sup>[7]</sup> Voyer<sup>[8]</sup> or Barboiu<sup>[9]</sup> have made significant contributions to the field of artificial crown-ether carriers or channels.

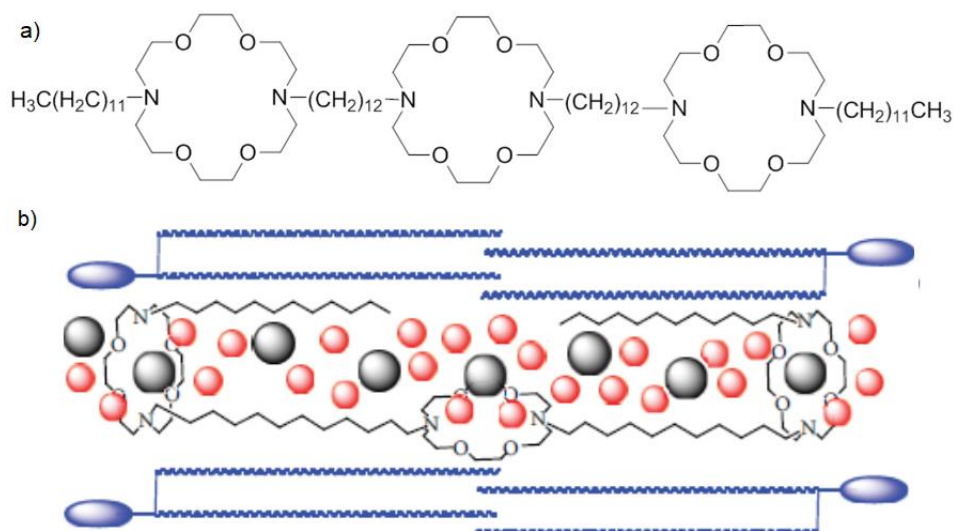


**Figure 1.** a) *Hydraphiles* as synthetic ion channels and b) schematic representation ion-channels translocation mechanism within the phospholipid bilayer *Adapted with permission from ref. 6g. Copyright 2013, Hindawi group.*

Gokel et al. have pioneered the field and we have to look back on the seminal development by of *hydraphiles*,<sup>[6a-c]</sup> a class of unimolecular amphiphilic ion-channels, composed from two diaza-18-crown-6 macrocyclic “head” groups for specific ion binding at the entry and ion-releasing at the end of the membrane as well as one “central relay” in the mid-plane of the membrane (Figure 1). The *hydraphiles* have been greatly explored *in vitro* for liposome-based ion transport assays, as well as *in vivo* for their biological activity, disrupting the cellular ion homeostasis in target bacteria or mammalian cells.<sup>[6d-f]</sup>



---

Natural KcsA  $K^+$  channels conduct ions at high rates with an extraordinary selectivity for  $K^+$  cations, excluding the  $Na^+$  or other cations. Biomimetic artificial channels have been designed in order to mimic the unique selectivity of KcsA  $K^+$  channels, but simple artificial systems presenting high  $K^+/Na^+$  selectivity are rare. The key to the design channels is to construct functional pores with a critical geometry for selective binding that allows free flow of ions. An optimal ion-bonding within the channel is needed for selectivity, while less friction with the channel structure is desired to increase the ion permeability.

Of special interest is structure-directed function of such channels and to control their build-up by self-assembly. The natural selectivity can be achieved by using simple crown-ether moieties pointing toward the channel core and directionally oriented by using self-assembly. Such a combination is hoped to result in a functional supramolecular organization of binding sites, collectively contributing to the selective translocation of cations along the pore. Barboiu et al. have developed directionally H-bonded urea crown-ethers, where the ion-translocation functions are associated to supramolecular self-assembly of the ion-channels. In these studies, significant membrane disruption is observed for hexyl-benzoureido-15-crown-5-ether **C5U6** or hexyl-benzoureido-18-crown-6- ether **C6U6**, that possess the ability to form columnar self-assembled ion channels. They show an extremely complex set of conductance levels for  $Na^+$  and  $K^+$ , respectively depending on their concentration into the bilayer membrane (Figure 2a,b).<sup>[9a,b]</sup> It is presumed that the entropic cost of cation dehydration must be optimal in the case where the macrocycle is dimensionally compatible with the diameter of cations for example  $Na^+$  with 15-Crown-5-ether and  $K^+$  with 18-Crown-6-ether.

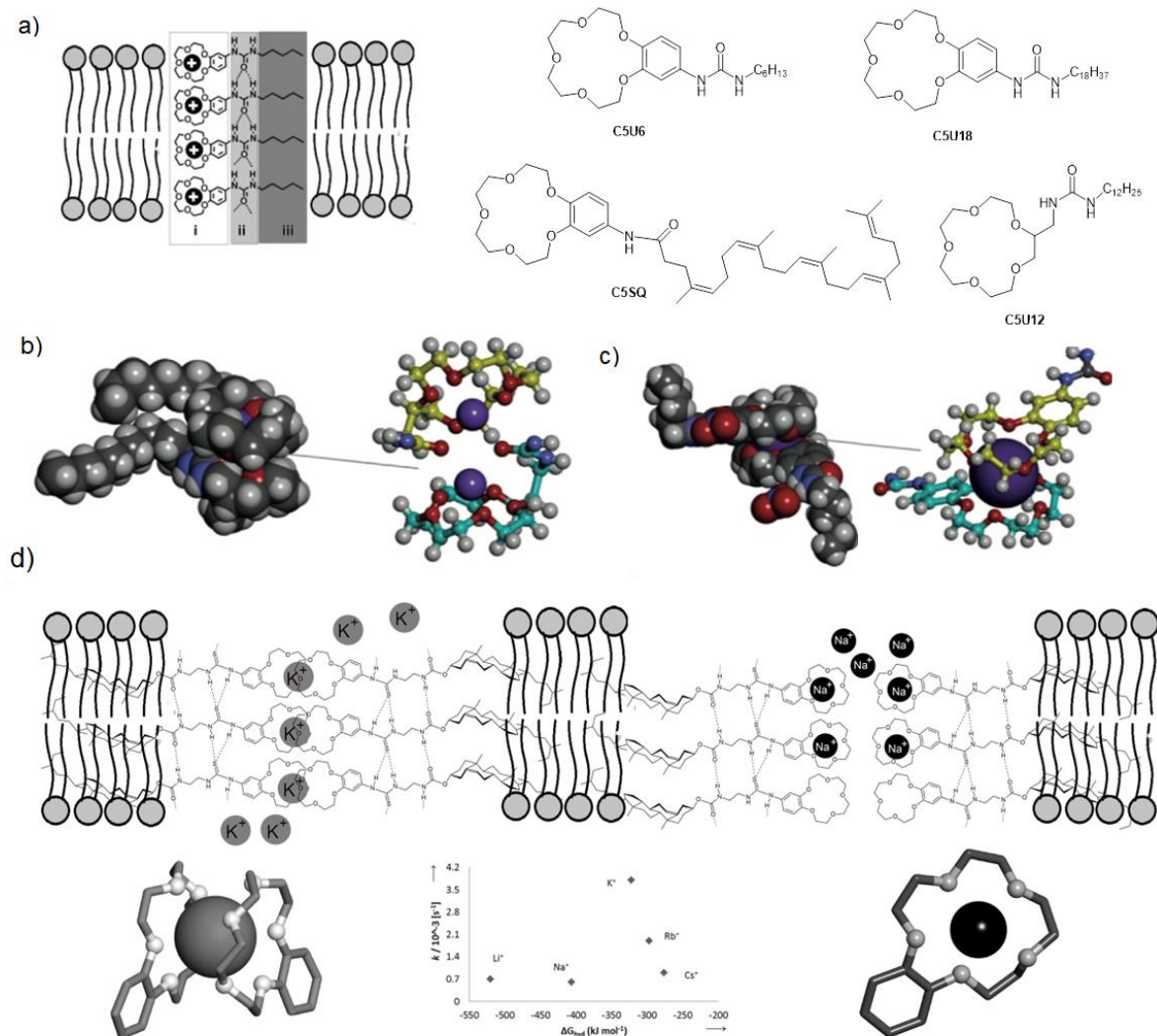


**Figure 2.** a) Structural encoded features of alkylureido-crown-ether channels: i) macrocyclic cation-binding sites, ii) directional hydrogen-bonding groups and iii) alkyl hydrophobic tails allowing integration within the bilayer membrane. Crown-ethers **C5U6**, **C5U18**, **C5SQ**, and **C5U12** and X-ray single-crystal structures of b)  $(C5U6)_2 \cdot K^+$  and c)  $(C5U12 \cdot Na^+)_2$ . d) Schematics of the possible organization of compounds in the bilayer resulting in the “double sandwich model” for  $K^+$  cations and macrocyclic binding of fittest  $Na^+$  cations. The first-order rate constants  $k$  for the transport of alkali cations through LUVs containing **C5Chol**.

It was recently discovered that unconventional sandwich-type binding toward  $K^+$  by 15-Crown-5-ether channels is responsible for their enhanced translocation inducing a passive polarization of the membrane. These channels are selectively responsive to the presence of  $K^+$  cation even in the presence of  $Na^+$ .<sup>[9c]</sup> From the conceptual point of view they express a synergistic adaptive behaviour: the addition of the  $K^+$  cation drives the selection and the construction of selective channels for the  $K^+$  cation that promoted its generation in the first place. This is a self-instructed

---

ion-channel system, where an ion induces itself the activation of its own selective translocation. Complementary studies by Barboiu et al. showed that, the mobility/fluidity of resulted channels inside of the bilayer membranes is required for the high adaptive translocation of cations *via* multivalent binding/release “jumping” between spatially closed macrocyclic relays. For example, flexible crown ethers **C5U12**, aggregating in bilayer membranes, favour six-fold coordinated  $\text{Na}^+$  cation at low concentration acting as carriers (Figure 2b), then turned into ten-fold coordination with  $\text{K}^+$  cation at high concentration acting as ion-channels (Figure 2c).<sup>[10]</sup> Higher mobility of hexyl-**C5U6**<sup>[9c]</sup> related to the relatively lower fluidities of Cholesteryl **C5Chol**<sup>[11a]</sup> or Squallyl-SQ **C5SQ**<sup>[11b]</sup> within bilayer membrane, favour the formation of highly dynamic and less rigid channel superstructure (Figure 2d). Cholesteryl **C5Chol**<sup>[11a]</sup> and Squallyl-SQ **C5SQ**<sup>[11b]</sup> compounds present an initial transport rates for  $\text{K}^+$  cations of  $k_{\text{K}^+}=3.9\cdot 10^{-3} \text{ s}^{-1}$  and  $k_{\text{K}^+}=87.5\cdot 10^{-3} \text{ s}^{-1}$ , (1:10 mol, compd: lipid) respectively. Under the same conditions, compound **C5U6** presents one order of magnitude higher initial transport rate of  $k_{\text{K}^+}=175\cdot 10^{-3} \text{ s}^{-1}$  for  $\text{K}^+$  cations. A kinetic selectivity of  $S_{\text{K}^+/\text{Na}^+}=58.3$  and a reasonable  $\text{EC}_{50}=15.8 \mu\text{M}$  for  $\text{K}^+$  ion had been achieved by compound **15SQ**.<sup>[11b]</sup>

Zeng and co-workers developed self-assembled  $\text{K}^+$  channels, with a  $\text{K}^+/\text{Na}^+$  selectivity of 9.8 and an  $\text{EC}_{50}=6.2 \mu\text{M}$  for  $\text{K}^+$  (Figure 3).<sup>[12]</sup> They strategically devised a monopeptide-based chiral synthon with a built-in directional hydrogen-bonding network with an A-D-A-D pattern. The channel-forming properties of **5F8** were confirmed by single channel current traces, recorded in both symmetrical and asymmetric baths. The system with monopeptide-based scaffold highlighted the tunable directional assembly of crown ethers. Their strategy with predefined directional assembly and an intrinsic high modularity in backbone provides an

evolutionary combinatorial strategy for rapid discovery of ion channels with optimized activity and selectivity. Intriguingly, **5F8** can transport  $K^+$  ion slightly faster than natural ion channel Gramicidin A does under similar conditions.

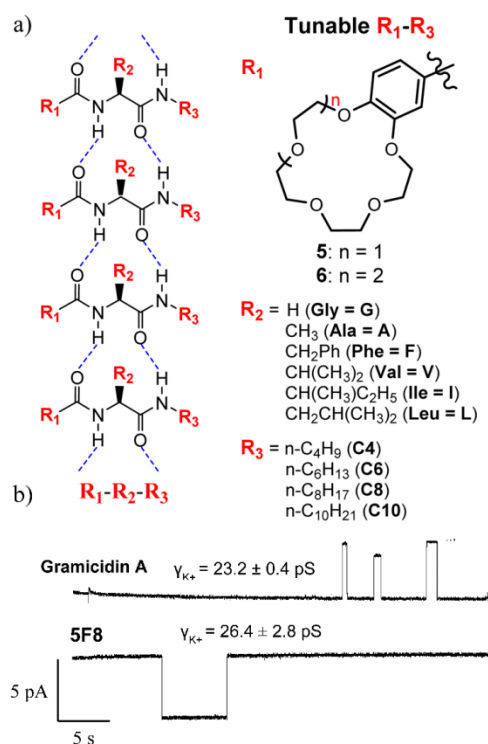


**Figure 3.** a) Combinatorial screening of supramolecular chiral synthons for efficient and selective ion channels discovery. b) Single channel current traces of (top) natural ion channel Gramicidin A recorded at 200 mV and (bottom) **5F8** recorded at  $-200$  mV, respectively. *Adapted with permission from ref. 12 Copyright 2017, American Chemical Society.*

Barboiu, Giuseppone et al. reported artificial channel formed by columnar self-assemblies of triarylamine-18-crown-6 ether compounds, **DC6T8**, which can translocate  $K^+$  cation through lipid bilayer membranes.<sup>[13]</sup> Distinct from other channels, the triarylamine pillars act as directional scaffolds for peripheral crown-ether moieties mutually self-assembled into columnar channels fitting with  $K^+$  cation-water wires, very similar to those observed in natural KcsA  $K^+$  channels and have been revealed by the X-ray crystal structures of **DC6TN** (Figure 4). This work extended the applications of triarylamines toward the construction of artificial biomimetic channels of directionally close-packed crown ethers.

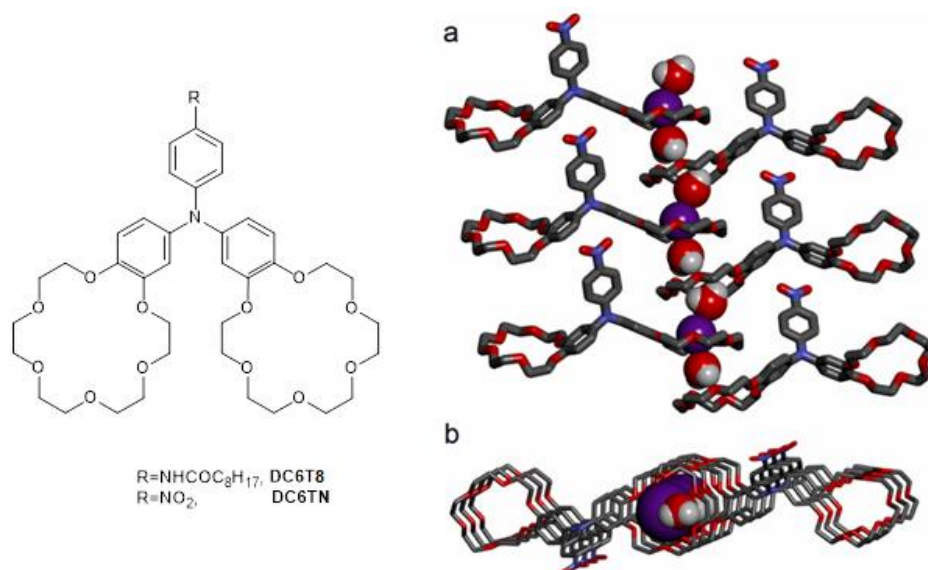


**Figure 4.** Chemical structures of triarylamine-18-crown-6 ethers **DC6T8** and **DC6TN** (left), and the  $\text{K}^+$  channel superstructure by alternation  $\text{K}^+\cdot\text{H}_2\text{O}$  wires along the  $b$ -axis (right, a) and the parallel alignment of crown-ether-triarylamine molecules along the  $a$ -axis (right, b) in crystal structures of **DC6TN**.

Natural ion channels gated between conductive (“ON”) and non-conductive (“OFF”) states in response to intracellular or extracellular stimuli are of significant interest for signaling, metabolism and immunity processes. Within this context, light-controllable supramolecular ion-channels have been reviewed by Hou et al.<sup>[14]</sup> Bao, Zhu et al. have developed crown-ether-based ion-channels to explore their structure-function relationship and photo-gating. They used the photo-isomerization of azobenzene to build light-gated azobenzene-*hydraphile*<sup>[15a]</sup> (Figure 5a) or H-bonded crown-ether ion-channels.<sup>[15b]</sup> The crown-ether **M1** containing a photocleavable *o*-nitrobenzyl group can operate within ion-channels to achieve full blockage when exposed to a light stimulus (Figure 5b). Before irritation, the self-assembled channel is able to transport  $\text{K}^+$  cation effectively; once irradiated at 365 nm with UV light for 10 min, the channel loses of up to 95% activity, due to the photo-cleavage of hydrophobic tail from recognition site.<sup>[15c]</sup> This report reaffirms the significance of the optimal membrane insertion of artificial channels and opens a new avenue to the light-gated synthetic channels.

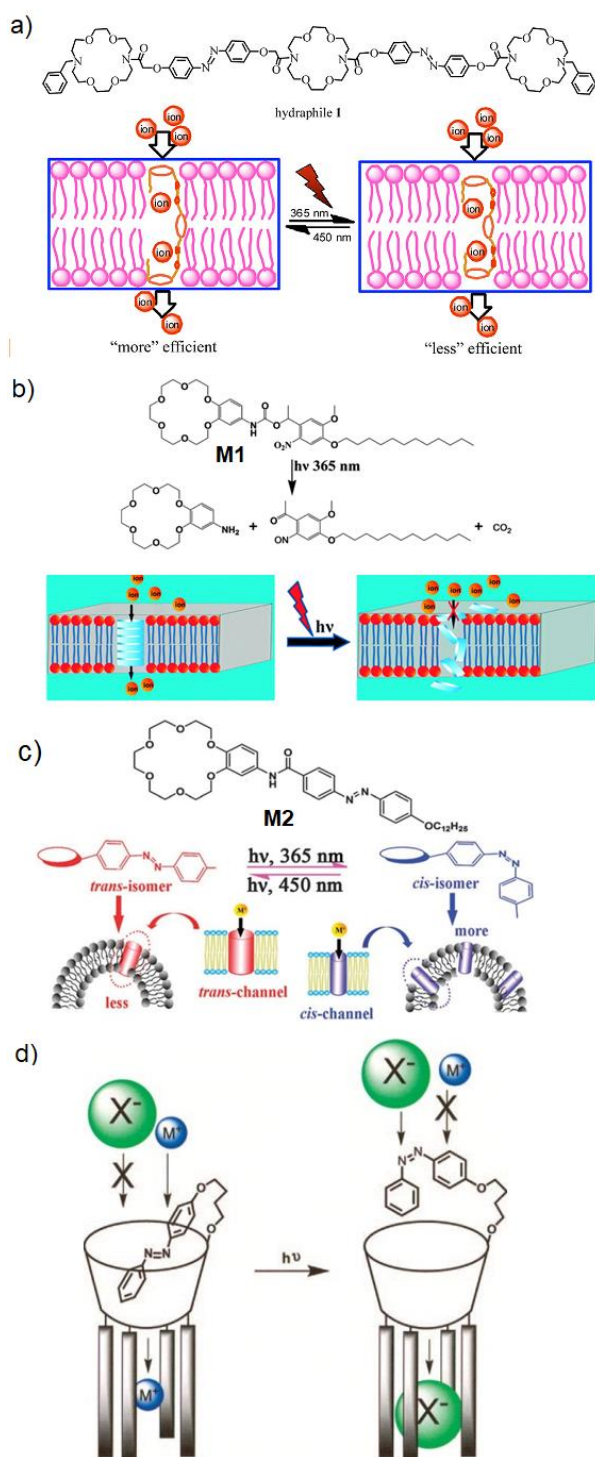


**Figure 5.** a) Structure of light-controlled *hydraphile 1* and its transmembrane ion transport mechanism. b) Deactivation of channel mechanism *via* photo-cleavage/disassembly of **M1** in lipid bilayers. c) Schematic diagram of compound **M2** as photo-switch resulting in cis/trans azobenzene-channels with different ion permeability. d) Schematic representation of the light switching cation/anion transport mechanisms through azobenzene-tethered  $\beta$ -cyclodextrin channel. Adapted with permission from ref. 15a,c,d Copyright 2013, The Royal Society of Chemistry. ref. 15e. Copyright 2008, American Chemical Society.

---

Zhu et al. synthesized the amphiphilic molecule **M2** comprising four structural motifs: 18-crown-6 ether as ion filter, hydrogen-bonding amide group to direct the channel architecture, photo-responsive azobenzene unit operating as a light-switch and alkyl tails enhancing lipophilic affinity toward bilayer lipids (Figure 5c)<sup>[15d]</sup>. Their design strategy turned out to be a success. Two ion-channel structures with different activities under different light wavelengths were observed by UV-visible and <sup>1</sup>H-NMR spectroscopies, thereby achieving the switching in K<sup>+</sup> permeability.

Gin et al. studied a light-regulated channel<sup>[15e]</sup>, inspired by previous findings that *trans*-azobenzene binds stronger to the β-cyclodextrin cavity (or “gate block”) than its *cis*-azobenzene counterpart, which offers an attractive opportunity for light-regulated Na<sup>+</sup> cation release.<sup>[15f]</sup> As expected, photo-irradiation indeed induce the formation of the *cis*-azobenzene, partially blocking the pore, reminiscent to inactivation of the gated nature channel.<sup>[15g]</sup> Moreover, when the “gate” was open, the channel inclined to attract more anions than cations (for instance, Cl<sup>-</sup> transport rate increase 2.5 times, while Na<sup>+</sup> transport rate weakened). They proposed that at open state, bulky hydrated anions species could make most use of the hollow channel cavity (Cl<sup>-</sup> > Br<sup>-</sup> > I<sup>-</sup>) and at closed state, the azobenzene-bound complex easily accepts smaller cations through cation-π interaction to reduce the dehydration energy expenditure (Figure 5d).

Liu, Hou et al. achieved *in situ* reversibly light-regulated supramolecular artificial channels.<sup>[16]</sup> Acylhydrazone-crown ether triad **1<sub>E</sub>** in *E* configuration was found to form ion-channels in bilayer membrane *via* intermolecular hydrogen-bonding and aromatic stacking interactions (“ON” status) (Figure 6a). Once irradiated under alternating 320 and 365 nm UV light, the ion channels *in situ* disassembled (“OFF” status), presumably resulting from the photo-regulated



*cis/trans* isomerization of the C=N bonds in the triad (Figure 6b). Notably, this photo-regulated isomerization can accomplish complete on/off gating (Figure 6c).

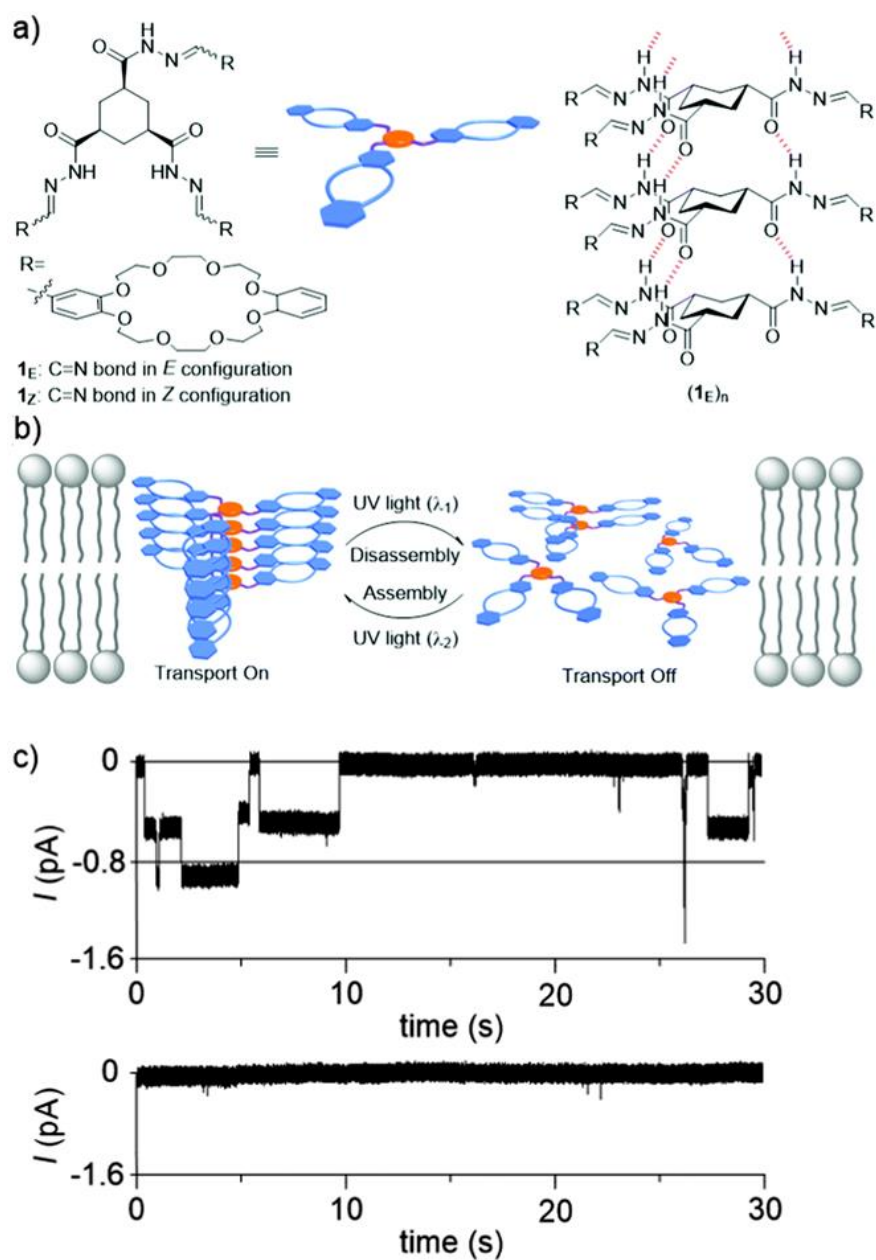


**Figure 6.** a) Chemical structures of  $1_E$  and  $1_Z$ , and proposed self-assembly of  $1_E$  to columnar ion channels, b) scheme for the ON/OFF gating of triad  $1_E/1_Z$ , and c) (top) current traces of  $1_E/1_Z$  at  $-100$  mV by irradiation with alternating 320 and 365 nm UV light and (bottom) without irradiation. Adapted with permission from ref. 16 Copyright 2017, Royal Society of Chemistry.

Mechanical motions can be used to construct specific devices for selective transport. Qu et al. reported an artificial molecular shuttle embedded into lipid bilayers that work as a *vehicle* for



ion transport.<sup>[17]</sup> The relatively active shuttle **[2]rotaxane 3** consisted of two components: a thread amphiphilic structure **T3** as a cable across the membrane, a dibenzo-24-crown-8 macrocycle **CE** acting like a wheel in interaction with three positive charged groups along the cable, and a benzo-18-crown-6  $K^+$  carrier shuttling along the thread. The ion transport activity of **[2]rotaxane 3** was significantly higher than the components **T3** and **CE**, confirming that the shuttle is the key factor for an efficient ion transport. (Figure 7)

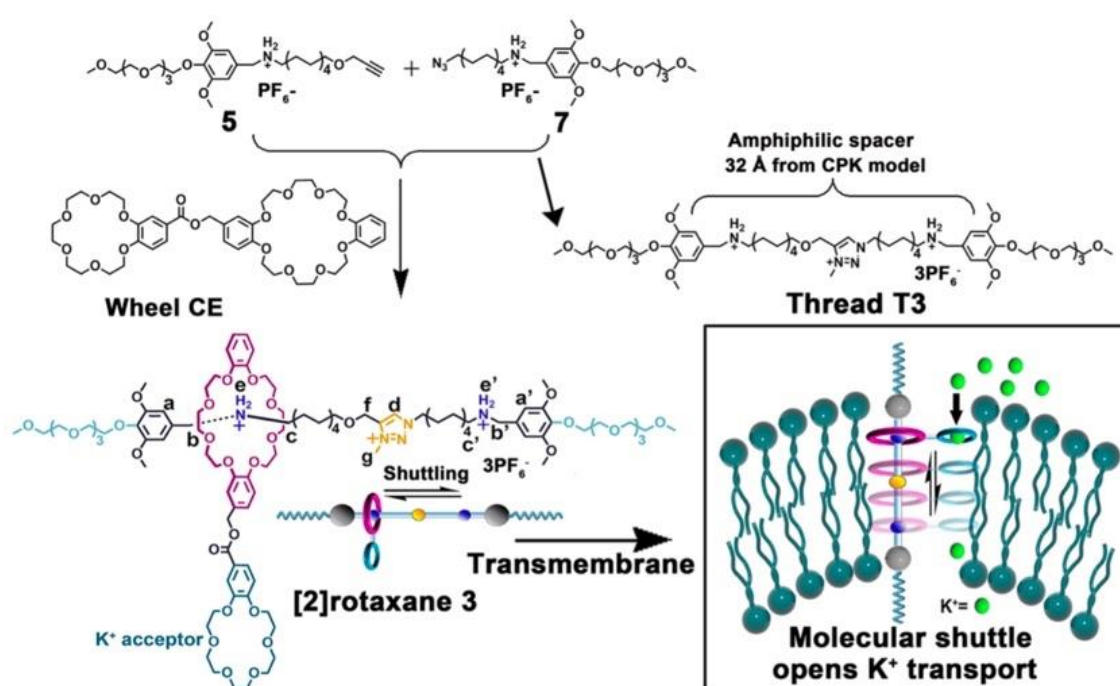


**Figure 7.** The self-assembly of **[2]rotaxane 3** is the key factor for an efficient ion shuttle transport mechanism Adapted with permission from ref. 17 Copyright 2018, American Chemical Society.

Zeng and coworkers used an unprecedented molecular motion related to an ion-fishing transport mechanism.<sup>[18]</sup> Unlike the common ion channels, ion fishers consist of hydroxyl-rich cholesterol groups as a rigid fishing rod, flexible alkyl chain-based fishing line and crown ether-based fishing bait/hook, which are highly modular. Among these high selective ion fishers, **MF6-C14** shows the excellent  $K^+/Na^+$  selectivity of 18 and an  $EC_{50}$  value of 2.5  $\mu M$  for  $K^+$  cation, while exceptionally do not transport  $Li^+$ .

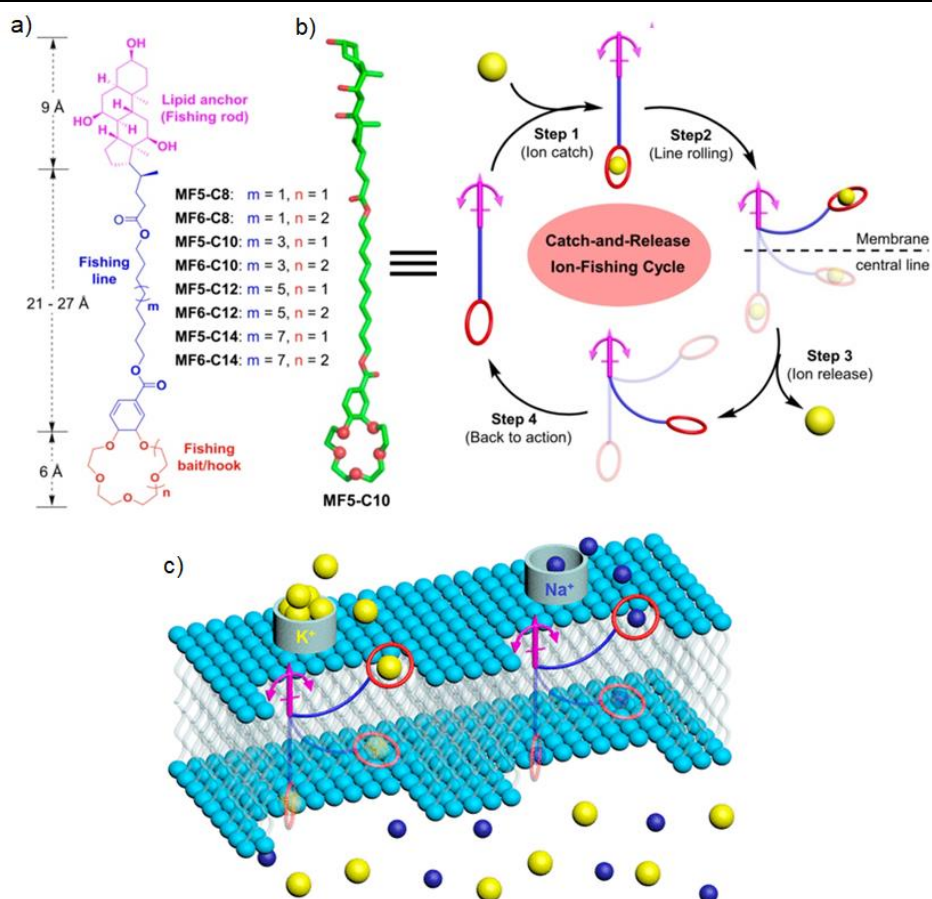


**Figure 8.** Molecular design of ion fishers MF5s and MF6s. (b) Computationally optimized structure of MF5-C10 and (c) Ion-fishing mechanism for ions catching-and-releasing through the membrane. Adapted with permission from ref. 18 Copyright 2019, American Chemical Society.

**Nanotube-Based Artificial Channels.** The rational design and skillful synthetic strategies have been used over the last decades, to full control over the internal diameter and external surface properties of the hollow nanotube architectures.<sup>[19]</sup> Ghadiri et al. have been pioneered the field, by tuning the cation transport efficiency and selectivity through cyclic peptide nanotubes (Figure 9).<sup>[20]</sup> The self-assembly of cyclic peptides into nanotubes with a hydrophilic cavity of  $\sim 7.5$  Å diameter was driven by a) the intermolecular hydrogen-bonding between amide moieties and b) the hydrophobic interactions between side chains and lipids. Interestingly, a peptide nanotube, CP1 showed an  $K^+$  flux of  $2.2 \times 10^7$  ions  $s^{-1}$ , three times faster than gramicidin A. This milestone accomplishment has laid down the foundation of a) self-assembly of a variety

of nanotubes with different inner hollow pore and external surface properties and b) the alternating alignment of donor and acceptor hydrogen-bonding for the construction of supramolecular channels. Later, Ghadiri tuned the cyclic peptides and demonstrated that functionalized cyclic peptides effectively mediate transmembrane transport of other metabolites like glucose<sup>[21a]</sup> or glutamic acid.<sup>[21b]</sup>

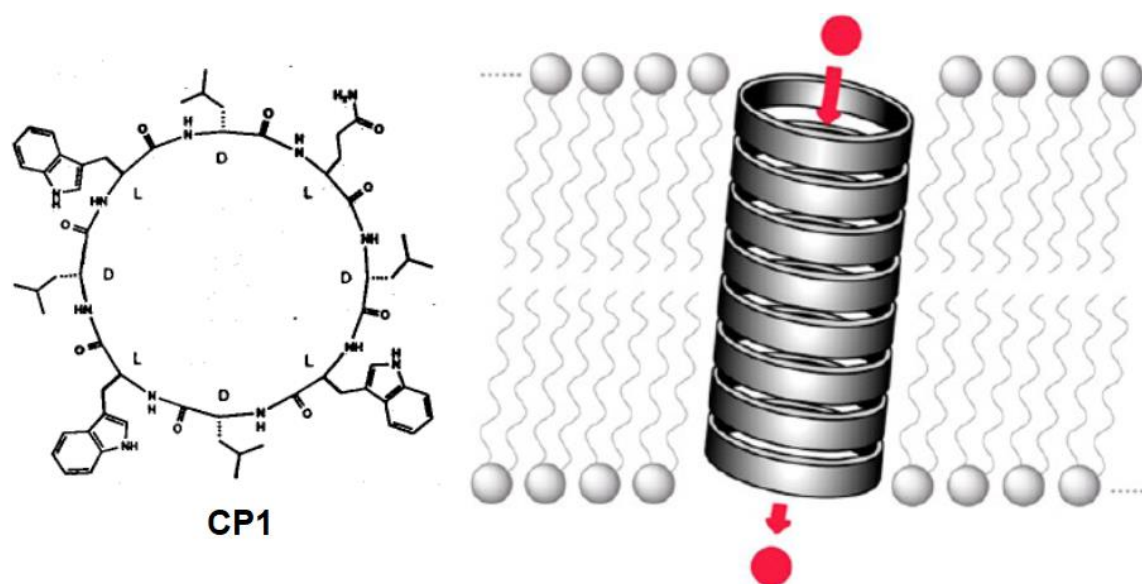


**Figure 9.** Chemical structure of cyclicpeptide **CP1** and its self-assembled tubular configuration in lipid bilayer membrane. Adapted with permission from ref. 19. Copyright 2019, American Chemical Society, 1994 Nature.

Gong and co-workers have built a variety of self-assembled nanotubes using aromatic oligoamides macrocycles.<sup>[1b,22]</sup> The shape-persistent aromatic oligoamides, stabilized *via* intramolecular hydrogen-bonding are self-assembled into *hydrophilic* tubular channels of ~8.3-8.5 Å in diameter, through intermolecular stacking (Figure 10a,b).<sup>[23]</sup> Intriguingly, two channels (**g1d** and **g1e**) show significantly high conductance up to  $770 \pm 30$  and  $890 \pm 52$  pS (0.5 M KCl), towards  $K^+$  cations in lipid bilayer membranes, comparable to that of  $\alpha$ -hemolysin (800 to 1000 pS) under similar conditions. Later, a new generation of aromatic oligoamides that form hydrophilic channels showed improved activities for transmembrane transport of protons.<sup>[24]</sup>

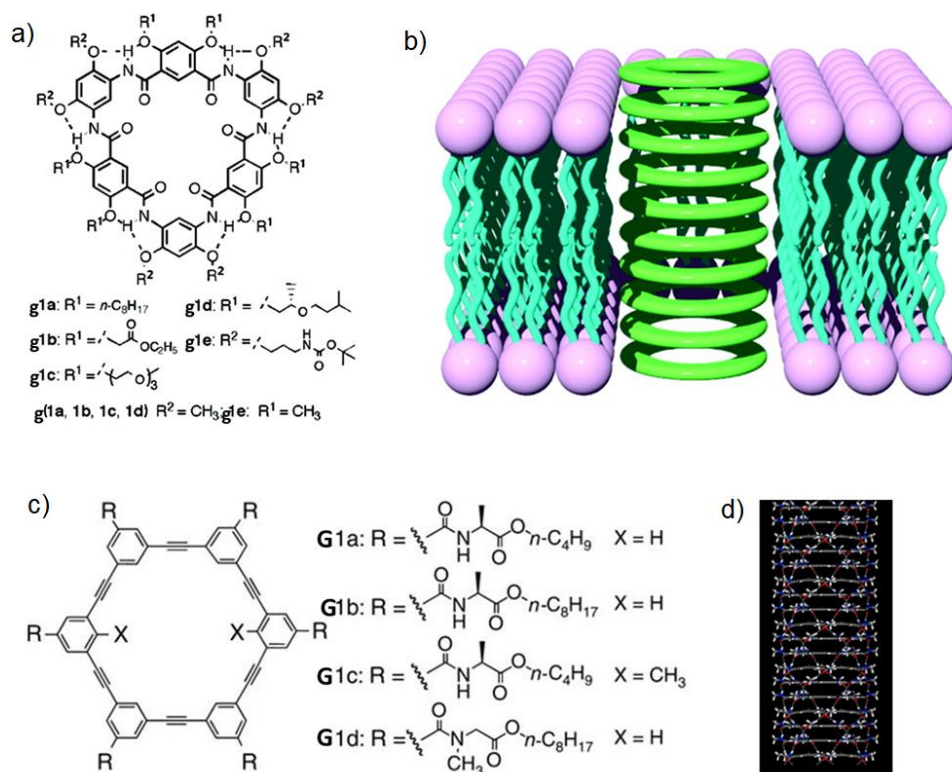


**Figure 10.** Chemical structures of a, b) cyclic oligoamides **g1a-g1e** and c, d) *m*-oligophenylethynyl OPEs **G1a-G1d** macrocycles and their corresponding nanotubular self-assembly within lipid bilayer membranes and theoretical models, respectively. Adapted with permission from ref. 22, 25 Copyright 2019, American Chemical Society.

Meanwhile, Gong et al. described other *hydrophobic* tubular pores formed *via* self-assembly of *m*-oligophenylethynyl (OPE) macrocycles with different inner pores and side chains.<sup>[25]</sup> The macrocycles self-assembled into hydrophobic helical tubular nanotubes with ca. 6.4 Å of diameter, driven by  $\pi$ - $\pi$  stacking between aromatic macrocycles and hydrogen-bonding between side chains, as supported by computational studies and experimental data. Without the smooth inner surface of CNTs, the stacked OPE macrocycles show very high-water permeability, up to 22% that of natural Aquaporin water channel AQP1 and exhibited extremely high ion pairs selectivity:  $P_{\text{H}^+}/P_{\text{K}^+} = 2000$ , while, no transport activity towards  $\text{Li}^+$  and  $\text{Na}^+$  ions was observed. Notably, the  $P_{\text{H}^+}/P_{\text{Cl}^-} = 3000$  of **G1a** surpass  $P_{\text{H}^+}/P_{\text{Cl}^-} = 19.7$  observed for natural proton influenza virus M2 protein channel. The high selectivity was attributed to the differentiated dehydration energies of ions based on molecular dynamic (MD) simulations. The

impressive investigations reported by Gong et al show the variety of nanotubes with either hydrophilic or hydrophobic cavities, can be used to transport both ions ( $H^+$ ,  $K^+$ ) and water molecules.

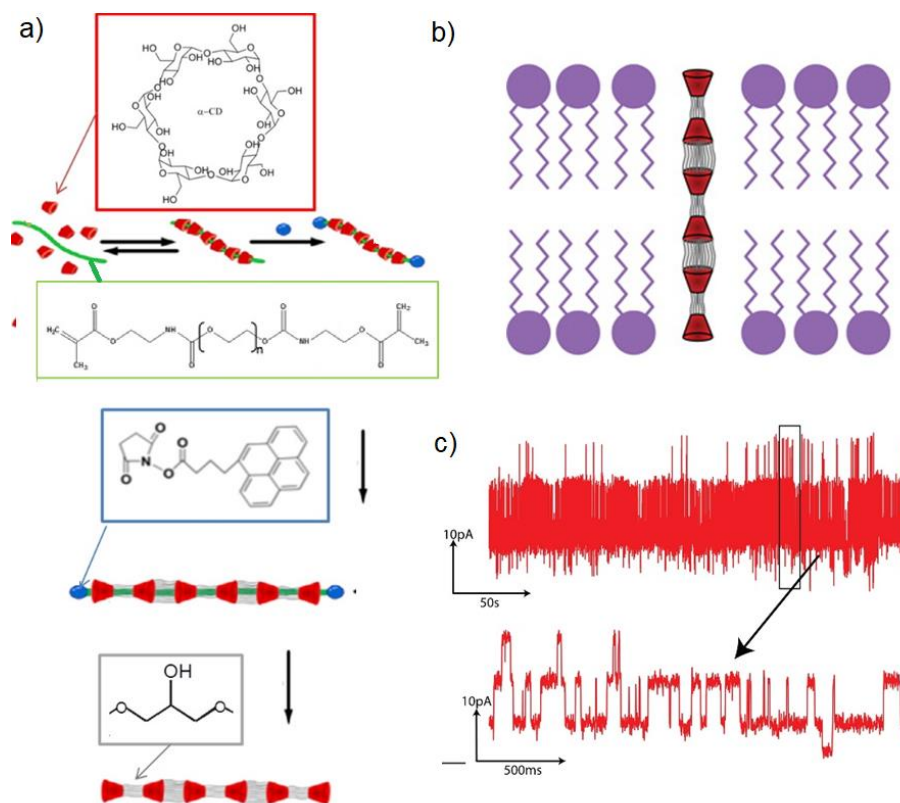


**Figure 11.** a) Synthesis of  $\alpha$ -cyclodextrin nanotubes-CDNTs, prepared by threading  $\alpha$ -cyclodextrin with  $\alpha$ - $\omega$  dimethacrylate PEO, end capping with pyrene-stoppers, gluing of the end rims by using epichlorohydrin and finally dethreading *via* hydrolysis of the axle. B) self-assembled tubular configuration and c) ion-conduction behaviors in lipid bilayer membrane of resulted CDNTs. *Adapted with permission from ref. 26c Copyright 2015, American Chemical Society.*

Recently, Jarroux et al. have reported a series of biomimetic cyclodextrin nanotubes constructed *via* a supramolecular bottom-up approach and explored their ion transport properties in bilayer membranes (Figure 11).<sup>[26]</sup> Polyrotaxanes were prepared *via* typical threading between  $\alpha$ -cyclodextrins and  $\alpha$ - $\omega$  dimethacrylate-PEO and capping with pyrene derivatives. Then the neighbouring  $\alpha$ -cyclodextrin rings were glued on their rims using epichlorohydrin. After hydrolysis and dethreading of inner  $\alpha$ - $\omega$  dimethacrylate PEO, various  $\alpha$ -cyclodextrin nanotubes



(CDNTs) were prepared. Electrical measurements with a nanopore setup showed the conductance of CDNTs up to  $0.0077 \pm 0.005$  nS, close to natural Gramicidin A. Later, the same group demonstrated that bigger  $\beta$ - and  $\gamma$ -cyclodextrins can also form CDNTs with various functionalization and they are able to transport  $K^+$  cations through the nanotubes. Interestingly, the CDNTs were determined to not present cytotoxicity towards various living cells, such as the MDA-MB231 cell line.

**Helical artificial channels** Many natural ion channels with ion transport regulation ability in living cells, are resulting from self-assembly of helix protein bundles, like the open pore conformation of KcsA  $K^+$  channels.<sup>[27]</sup> This inspires the exploration of various helical supramolecular artificial channels.

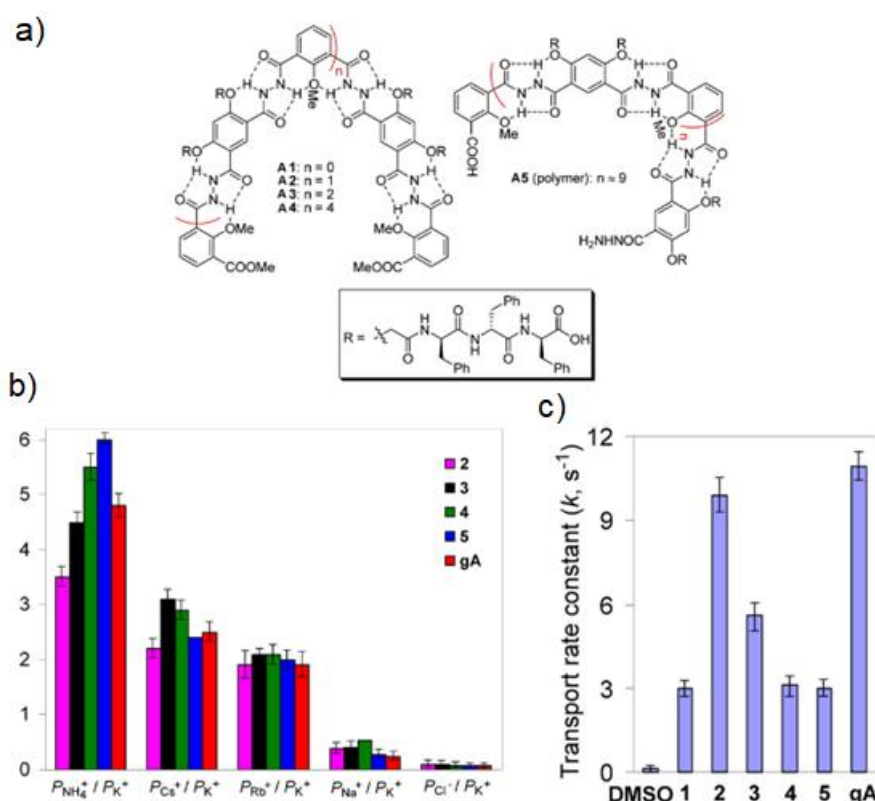


**Figure 12.** a) Chemical structures of A1-5, B) Permeability ( $P$ ) ratios through the channels formed by A2-5 and gA, revealing the selectivity of the helical channels, and c) Kinetic  $Tl^+$  cation transport rate constants from normalized stopped-flow fluorescence intensity of A1-5. Adapted with permission from ref. 28 Copyright 2014, American Chemical Society.

Within this context, Li, Hou and co-workers reported a class of hydrogen-bonding tripeptide-armed helical hydrazides **A1-5**, presenting transport activities, whose selectivity rival or even outmatch the natural Gramicidin A, under identical conditions (Figure 12). According to the stopped-flow experiments the transport efficiency towards  $\text{Tl}^+$  cation of **A2** acting as a unimolecular channel in membranes is comparable to that of Gramicidin A.<sup>[28]</sup>

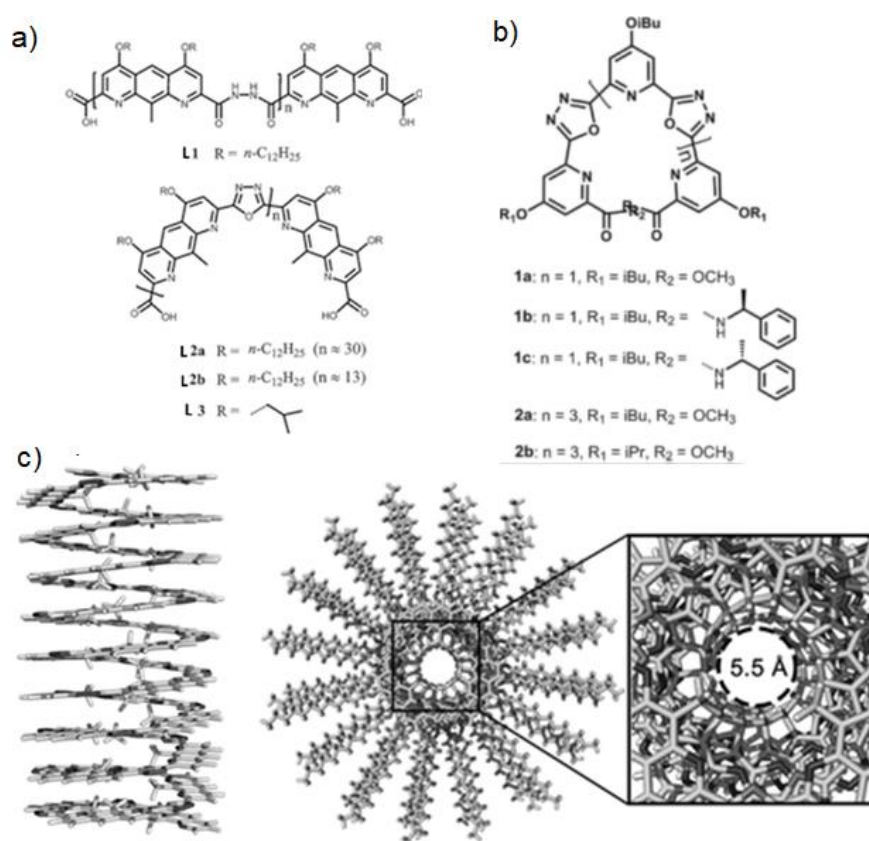


**Figure 13.** Chemical structures of helical foldamers a) **L1-3** and b) **1a-c**, **2a,b** and c) lateral and top views of modelled helical channels with a pore of 5.5 Å. Adapted with permission from refs. 29 Copyright 2016, 2017, Wiley.

In 2016, Liu, Dong et al. rationally designed a class of novel helical foldamers with expressively long lifetime channels towards protons and cations in bilayer membranes.<sup>[29a]</sup> MD simulations showed that the appropriate pore size of 5.5 Å renders these channels suitable for conducting ions with a perfect length of helix **2a** (3.3 nm), matching the thickness of lipid bilayer (3.5 nm) well enough to span the membrane (Figure 13b). Intriguingly, these helical macromolecular

---

channels exhibited exceptional stability in planar lipid bilayer experiments (tens to hundreds seconds), even superior to natural Gramicidin A ( $< 2$  s), under identical conditions. Shortly, the same group reported narrowest channel-forming helical foldamers self-assembling into artificial ion channels via aromatic stacking and showing a remarkable  $K^+/Na^+$  selectivity up to 22.5 and an  $EC_{50}$  value of  $4.1 \mu M$  for  $K^+$  cation for the transport through channel **2b** in bilayer membrane (Figure 13b).<sup>[29b]</sup> To some extent, these well-designed self-folded helical channels mimic the formation of protein channels, giving potentially interesting scenarios on structure-function relationship of natural ion channels.

Discovered in 1960s, G-quadruplexes are tubular architectures arising from stacks of G-quartets, superstructures formed *via* square planar hydrogen-bonding of four guanines and stabilized in the presence of a  $K^+$  cation template.<sup>[30]</sup> The inherent tubular hollow cavity in G-quadruplexes held the promise for the application as supramolecular artificial ion-channels. Matile et al. was the first to propose to use the self-assembled nucleobases as potential components to build supramolecular ion-channels and performed a model study to construct artificial barrel-stave G-quadruplexes *via* hydrogen-bonding and base stacking.<sup>[31]</sup> Shortly, Davis et al. reported the single crystal structures of a lipophilic G-quadruplex formed by stacking of two twisted  $G_8-K^+$  octamers coordinating three  $K^+$  and one  $Cs^+$  cations along its central axis leading to the formation of a solid state well characterized cation channel that potentially may be applied to artificial ion channels (Figure 14a).<sup>[32a]</sup> Later in 2006, Davis and colleagues developed a combined strategy of non-covalent self-assembly and covalent capture to prepare a unimolecular G-quadruplex **G4** over two steps, from a lipophilic guanine **G3** using templating  $K^+$  cations and ring closure metathesis reaction to form a unimolecular G-quadruplex **G4** acting



as a synthetic transmembrane ion transporter.  $^{23}\text{Na}$  NMR experiments clearly showed for the first time the efficient transport of  $\text{Na}^+$  through G-quadruplex **G4** superstructures, that can be detected within lipid bilayer membranes. [32b]

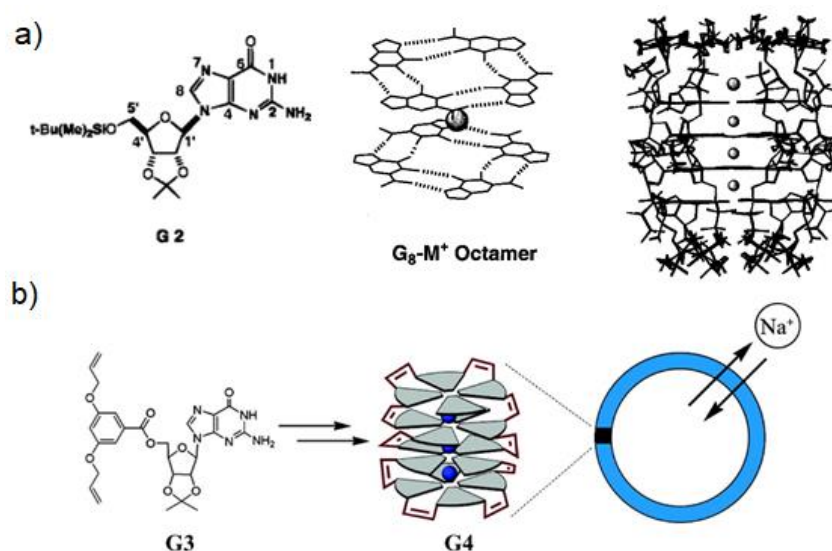


**Figure 14.** a) Chemical structure of lipophilic guanosine **G2** and  $\text{G}_8\text{-K}^+$  octamer and G-quadruplex-ion-channel superstructures; b) Schematic preparation of unimolecular G-quadruplex **G4** and its  $\text{Na}^+$  transport. Adapted with permission from refs. 32 Copyright 2000, 2006, American Chemical Society.

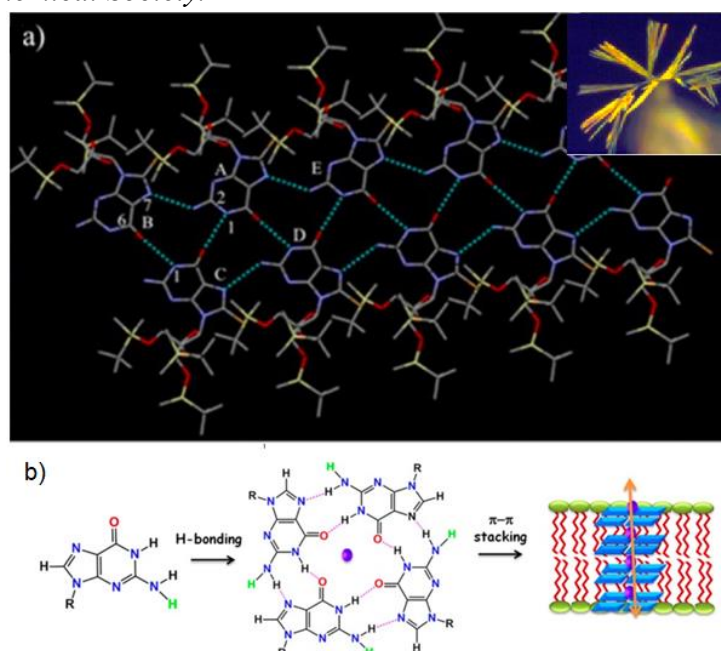


**Figure 15.** a) Ribbon-type H-bonding pattern in single crystal structure of lipophilic **BrG** displaying birefringence in polarized light; b)  $\text{K}^+$  cation templated **BrG**-quartet structures and their functional stacking in bilayer membranes Adapted with permission from ref. 33 Copyright 2018, Wiley

Recently in 2018, Dash et al. designed a lipophilic tert-butyldimethylsilyl-bromo-guanosine **BrG** which does not form G-quartets in the absence of cation template, but displays H-bonding ribbon patterns with birefringence in polarized light (Figure 15a).<sup>[33]</sup> The lipophilic chains in **BrG** protect the  $K^+$ -templated G-quadruplex channels *via* hydrophobic encapsulation in bilayer membranes. The traces of single-channel recordings by patch-clamp confirmed the formation of ion channels transporting the  $K^+$  cations through membranes (Figure 15b).

Matile et al. employed self-assembly of  $\pi$ -stacked folate rosettes to construct ion-channels.<sup>[34]</sup> Different from G-quadruplex, the formation of rosette folate-quartet can occur in the absence of a templating  $K^+$  ions, for which a maximum  $K^+$  single-channel conductance of  $g_{MAX} = 21$  pS and an  $EC_{50} = 0.23$  M have been obtained. Interestingly, the formed ion channels exhibited ohmic, long-lived, cation selective (Eisenman I) transport ability (Figure 16).

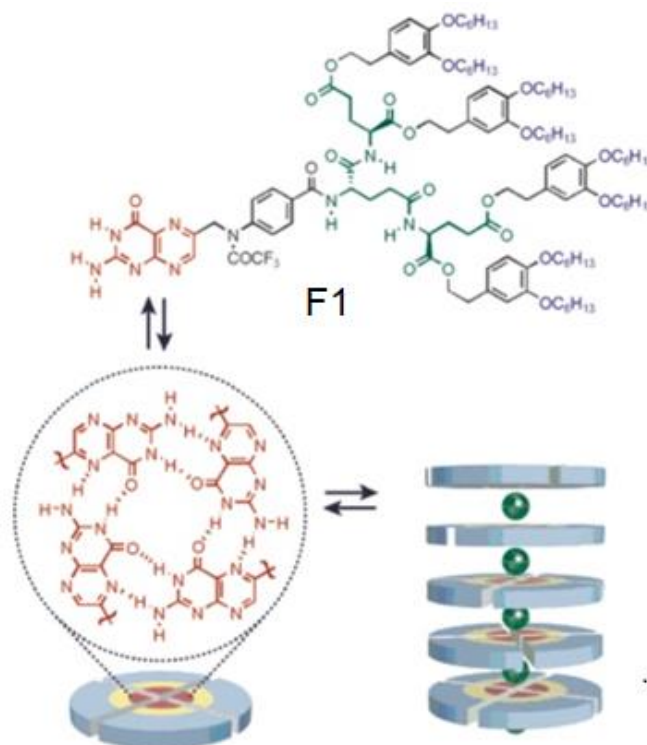


**Figure 16** Self-assembly of dendritic folate **F1** into F-quartet and subsequent self-stacking into F-quadruplex. Adapted with permission from refs. 34 Copyright 2006, American Chemical Society.

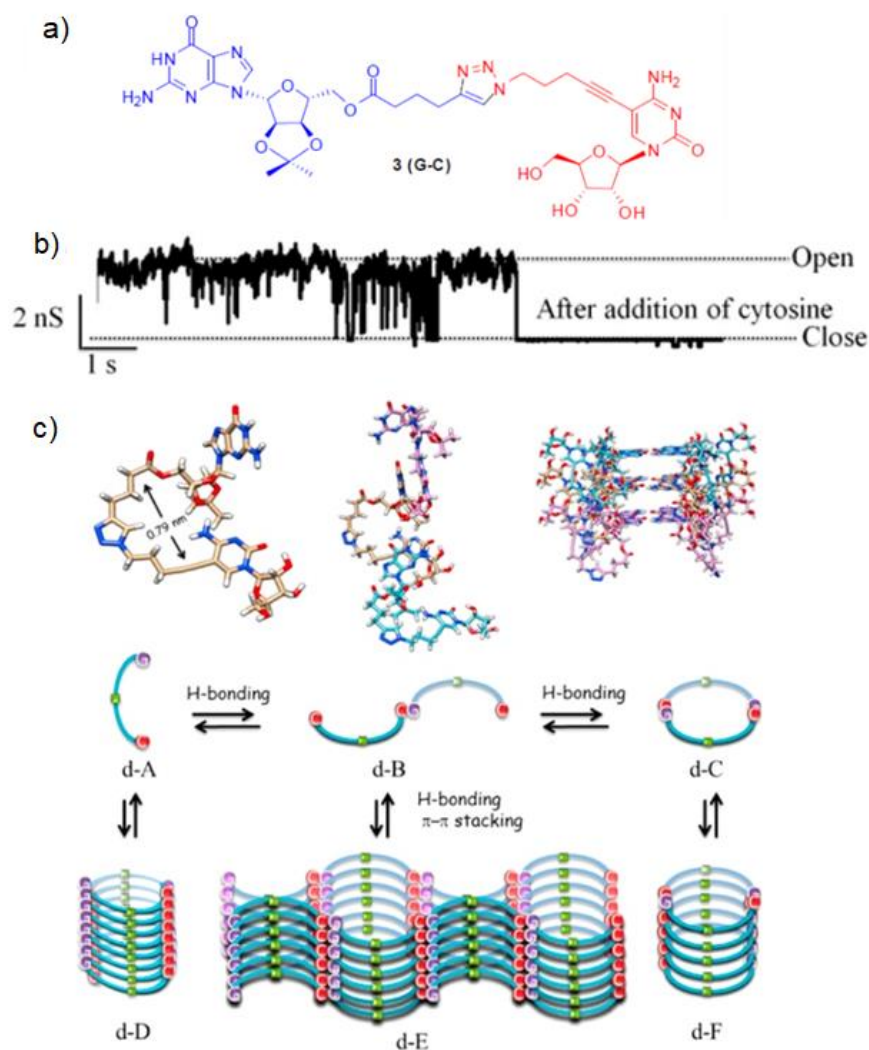


**Figure 17.** a) Chemical structure of dinucleoside **3(G-C)**; b) ion-conduction activity of ion-channel **3(G-C)** and its blockage by using cytosine; c) possible self-assembly modes of dinucleoside **3(G-C)** in lipid bilayer membranes. *Adapted with permission from ref. 35 Copyright 2006, American Chemical Society.*

In 2015, Dash and coworkers developed an artificial ion channel containing guanosine (G) or cytosine (C) bola-amphiphiles.<sup>[35]</sup> Due to the  $\pi$ - $\pi$  stacking of nucleobases and the hydrogen-bonding between guanosine and cytosine, the G-C bola-amphiphiles self-assemble into stable helical **d-D**, “barrel-stave” **d-E** or aggregated pores **d-F** nanostructures, respectively. Patch-clamp experiments were performed to confirm the formation of G-C channels, with 2.9 nS conductance for the transport of  $K^+$  cations across a lipid bilayer, that can be blocked by adding nucleobase cytosine.

**Metal organic architectures-based artificial channels.** One of the most common design strategies for synthetic ion channels is the use of organic molecules as structural scaffold and selectivity filter for the channel<sup>[36]</sup> Most of reported artificial ion channels are composed of organic molecules, but after flourishing development of metal-organic architectures,<sup>[37]</sup> the first lipophilic coordination complexes presenting ionic conductance states in bilayer membranes have been reported during the last decade.<sup>[38,40,41, 44]</sup>

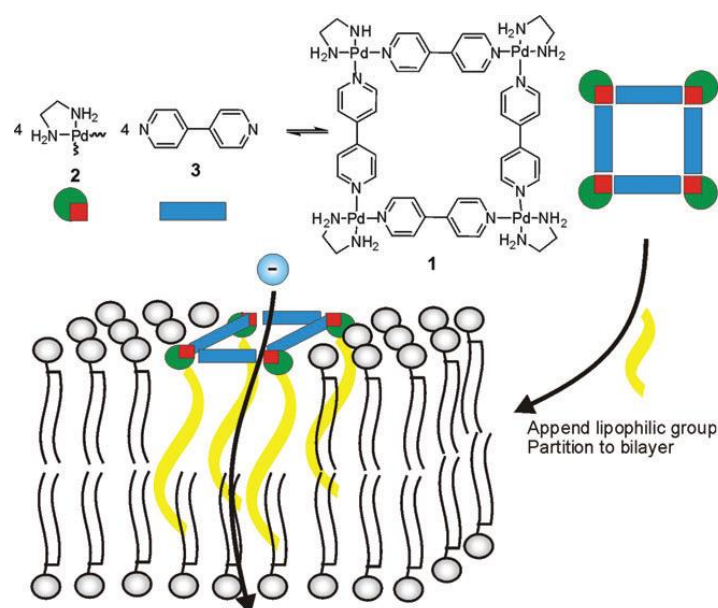


**Figure 18.** Self-assembled metallo-supramolecular channel based on a lipophilic ethylenediamine  $\text{Pd}^{2+}$  square complex. *Adapted with permission from refs. 38a Copyright 2007, Royal Chemical Society.*

Fyles et al.<sup>[38a]</sup> was pioneering the field and incipiently demonstrated in 2007 the efficiency of self-assembled metal-organic complexes for proton/cation transport across lipid bilayers. They started to construct ion-channels based on a lipophilic Fujita's square complex (Figure 18),<sup>[38b]</sup> but it was showed that the lipophilic  $\text{Pd}^{2+}$  complex is capable of forming very large supramolecular channels with internal pore diameters of 10 nm and composed of several  $\text{Pd}^{2+}$  centers. This was the starting point to explore the structural and functional features of this new type of synthetic metal-organic polyhedral channels.

Kim et al. introduced in 2008 a metal-organic polyhedral **MOP-18**, prepared from isophthalate and  $\text{Cu}^{2+}$  at room temperature<sup>[39]</sup> as an unimolecular-type channel,<sup>[40]</sup> which transports both proton and alkali cations without discrimination, *via* a channel mechanism, as confirmed by voltage-clamp experiments with ohmic long-lived currents. **MOP-18** is a stable hydrophilic cuboctahedron (diameter of the cavity of 13.8 Å) with two types of apertures (diameter of 3.8 Å and 6.6 Å) and a lipophilic outer shell allowing spanning along the lipid bilayers (Figure 19). This long-live ion channels are comparable to that of Gramicidin A and its cation selectivity follows Eisenman sequence XI, which is attributed to the cation- $\pi$  interactions between **MOP-18** and cations.

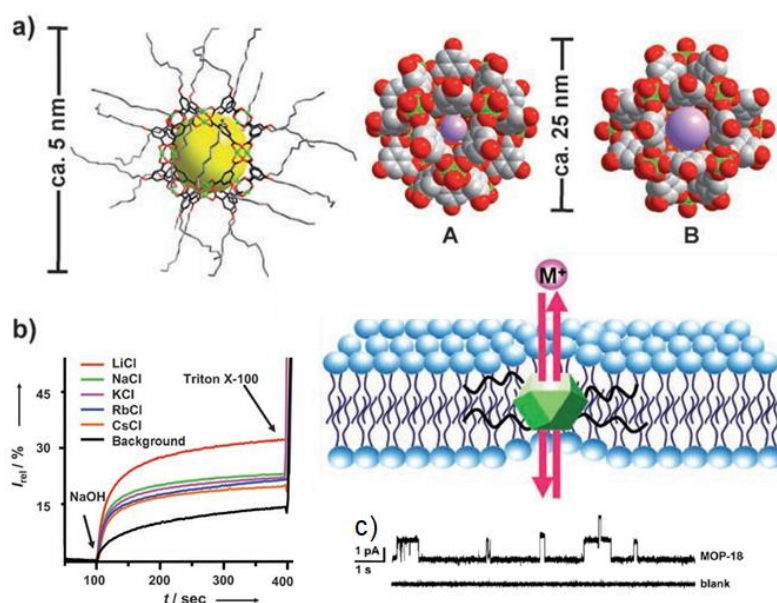


**Figure 19.** a) Metal-organic polyhedral **MOP-18** and its two types of apertures; b) HPTS assays showing the ionic transport and c) typical current profile measured with and without **MOP-18** at +60 mV in 2 M KCl showing the formation of ion channels in lipid bilayer membranes. *Adapted with permission from ref. 40 Copyright 2008, Wiley-VCH.*

Later in 2017, Furukawa et al. developed a  $\text{Rh}^{2+}$ -organic cuboctahedra with switching ion-channel conductances, corroborated with ion adaptive transporting pathways between two different triangular or square apertures of the cuboctahedra.<sup>[41]</sup> These  $\text{Rh}^{2+}$ -organic cuboctahedras self-assembled from dirhodium units and 1,3-benzene-dicarboxylate



functionalized with different alkoxy chains to increase lipophilicity. The length of the alkoxy chains played an important role in the transport properties by tuning pore opening time of each conductance of channels in bilayer membrane. In addition, the selectivity can be regulated: the  $\text{Rh}^{2+}$ -**MOP** transport  $\text{Ca}^{2+}$  divalent cations, while the  $\text{Cu}^{2+}$ -**MOP** transport monovalent cations.<sup>[41]</sup>

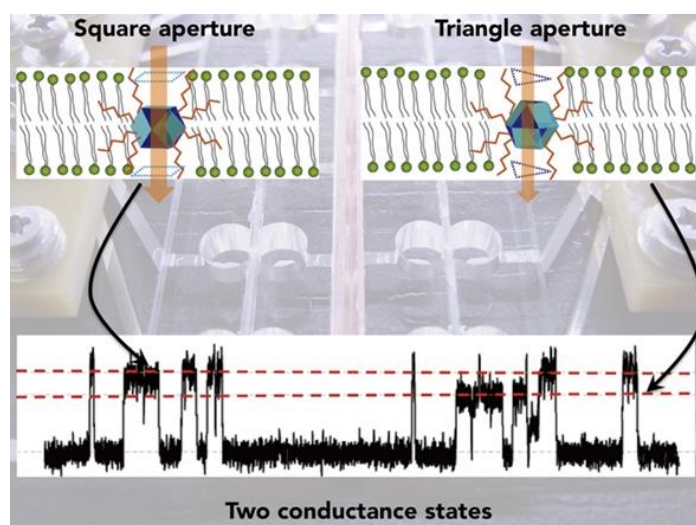


**Figure 20.** Schematic illustration of channels with multiple conductance states for a synthetic two-pore  $\text{C}_{14}\text{RhMOP}$  cuboctahedra channel and single conductance for each aperture. *Adapted with permission from ref. 41 Copyright 2017, Elsevier.*

Barboiu et al. reported that ion-channels showing ionic conductances through membranes can be formed from the spherical metal-oxide macroanions **Mo<sub>132</sub>**,  $[\{(\text{Mo}^{\text{VI}})\text{Mo}^{\text{VI}}_5\text{O}_{21}(\text{H}_2\text{O})_6\}_{12}\{\text{Mo}^{\text{V}}_2\text{O}_4(\text{CH}_3\text{COO})\}_{30}]^{42-}$  **POM1a**<sup>[42]</sup> and  $[\{(\text{Mo}^{\text{VI}})\text{Mo}^{\text{VI}}_5\text{O}_{21}(\text{H}_2\text{O})_6\}_{12}\{\text{Mo}^{\text{V}}_2\text{O}_4(\text{SO}_4)\}_{30}]^{72-}$  **POM2a**<sup>[43]</sup> encapsulated by dimethyldioctadecylammonium ( $\text{DODA}^+$ ) cationic surfactants.<sup>[44]</sup> The connection of the mentioned building units leads to the formation of 20  $\{\text{Mo}_9\text{O}_9\}$  crown-ether-type pores, alkali cations like ones can enter the capsule cavity. The concentration-dependent transport and the unusual sequence cation-selectivity in this system are the important proofs that the ions are transported inside the capsule. The observed permeability differences between the acetate-type **POM1a** and the sulfate-type **POM2a** capsules highly argues for

structural constraints of the ions interacting with the inner surface of the capsule during their transport. Altogether, this work demonstrates the potential of the investigated porous nano-architectures as interesting biomimetic ion channel systems.

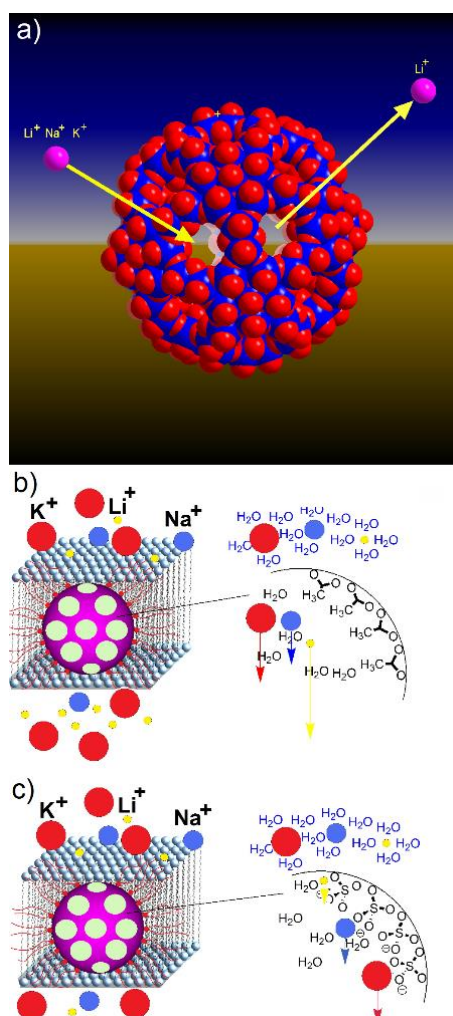


**Figure 21.** a) Spherical Porous **Mo<sub>132</sub>** Metal-Oxide DODA encapsulated Capsules. Comparison of  $\text{Li}^+$  (yellow),  $\text{Na}^+$  (blue) and  $\text{K}^+$  (red) cation transport b) the hydrophobic “acetate type” **POM1a** and c) the hydrophilic “sulphate type” **POM2a** clusters through the lipid bilayer membrane. *Adapted with permission from ref. 44 Copyright 2015, Wiley.*

Pyrogallolarenes are tetrameric aromatic macrocycles that could self-assemble depending on the nature of the alkyl side-chains, either as nanotube or as bilayer hexameric pore architectures, that can be inserted within bilayer membranes when pore formation was observed.<sup>[45]</sup> Their activities are significantly different from each other, reminiscent with other adaptive dynamic types of pores (Figure 22a). The assembled forms of pyrogallolarene **Pg6** significantly affect

the transport activity in phospholipid bilayers as reported by Gokel et al. Pyrogallolarene **Pg6**, isolated in bilayer form, is inactive, while once sonication in DMSO, it displayed reversible conductance properties over a wide range of potentials. In addition, the same group developed 3-pentyl and 4-heptyl pyrogallolarenes **Pg2** and **Pg3**, both of which were membrane active. For 3-pentyl pyrogallolarene **Pg2**, stacking of hexameric units of (**Pg2**)<sub>6</sub> into nanotube in phospholipid bilayers. The authors proposed that self-assembly of **Pg3** was different from that of **Pg2**, but did not provide its organization in lipid bilayers.

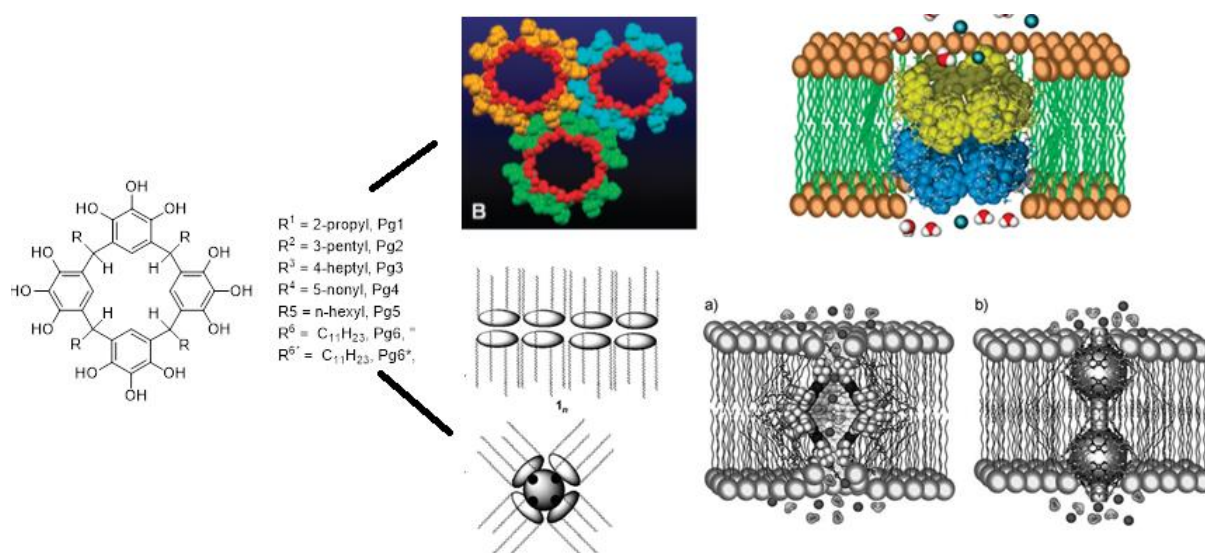


**Figure 22.** Chemical structures of pyrogallol[4]arene **Pg1-6**, (top) hexameric channels depicted in CPK in single crystal structures of **Pg5** and bilayer pore formation of **Pgn** and (bottom)  $\text{Cu}^{2+}$ -seamed pyrogallolarene capsule **Pg6-Cu** and its assumed single-capsule and double-capsule organization for the formation of pores within the bilayer membrane. Adapted with permission from ref.45a. Copyright 2009, Royal Society Chemistry and from ref. 46 Copyright 2009, Wiley VCH.

Based on these observations, Gokel et al. further introduced branched (metallo)pyrogallol[4]arene into the field of artificial ion channel.<sup>[46]</sup> Copper-seamed pyrogallolarene capsule **Pg6-Cu** formed active artificial channels towards  $\text{Na}^+$  and  $\text{K}^+$  ions in phospholipid bilayers. The authors postulated two possible mechanisms for the transport activity: single-capsule and double-capsule organization of capsule **Pg6-Cu** (Figure 22b).



---

### 3. Supramolecular artificial anion channels

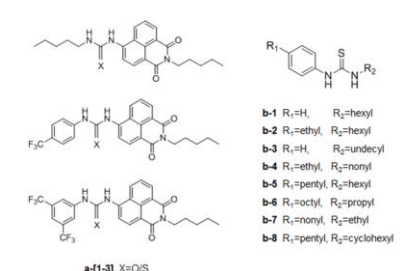
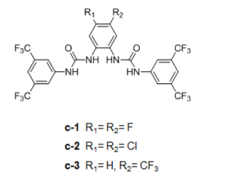
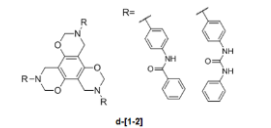
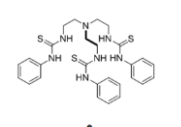
It's generally known that ion transport through membrane can be facilitated, mainly either *via* carrier or channel mechanisms. The strategies to construct synthetic carriers or self-assembled channels are quite different. For anion carrier fabrication, it is frequently required a cooperative hydrogen-bonding···anion or  $\pi$ ···anion with electrostatic interactions for an optimal anion binding in a suitable framework surrounded by lipophilic out-shell to easily fuse within the membrane lipids.<sup>[47b]</sup> In channel superstructures, arrays of ion-recognition sites are supposed to be closely aligned along the channel direction, so that ions can freely hop from one binding site to the next in site, as the permeation and ion selectivity are both regulated by the optimized ion binding strength at these sites.<sup>[48]</sup> So far despite a variety of self-assembled ion channel reports available, the design of synthetic channels with repeating ion-recognition sites is still challenging, especially for small-molecule based ion channels due to their poorly preorganized geometry of individual molecules and the lack of well-arranged binding sites.<sup>[49]</sup>

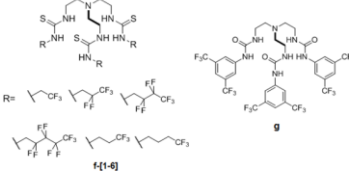
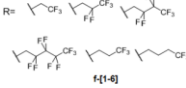
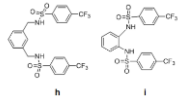
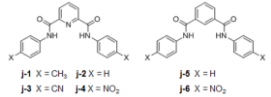
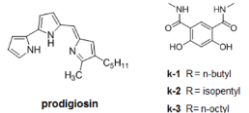
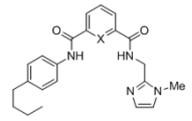
**Channel scaffold design inspired from various ion carriers.** Simple molecular receptors transferring anions through bilayers membranes and operating *via* a carrier mechanism inherit various advantages like easy accessibility in large quantities, tunable easy functionalization and amazing properties. Several reviews have been published over the past years concerning their synthesis and membrane transport applications of anion receptors or their use as building blocks for active medical applications.<sup>[48]</sup> The expectations are related to compensate the transmembrane charge imbalance caused by cation/proton transport which creates a positive potential outside the cell membrane with anion symport which is electrochemically transported out of the cell. Table 1 summarizes a few non-exclusively molecular structures documented in

---

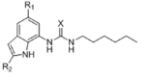
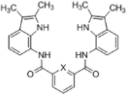
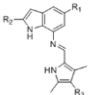
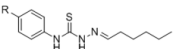
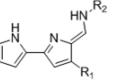
recent literature as active anion carrier molecules from which we may take some hints for rational design of channel with targeted scaffolds and functionality. The key strategy to design anion carriers from simple molecular components starts with their functionalization. So far, the combination of selective anion binding *via* hydrogen-bonding, ion-pairing, anion-dipole interaction or anion- $\pi$  interactions are used to create synergetic anion encapsulation and recognition functions. The use of electron-withdrawing groups can increase the anion binding and translocation. Numerous studies have identified lipophilicity (generally in quantitative representation as  $\log P$ ) as a major contributing factor in the transport activity.<sup>[40, 52]</sup> In general, more potent transport activity corresponds to higher  $\log P$  value. Nevertheless, there exists an upper limit beyond which transport efficiency and compound affinity toward lipids would no longer correlate.<sup>[51, 63]</sup> Lipinski's rule also suggests a  $\log P$  value at around 5 for drug-like transport systems with therapeutic potential<sup>[80]</sup>. For instance, introducing fluorination into compound design may result in stronger backbone-lipid interactions and hence, higher lipophilicity with better partitioning into the lipid bilayer, which has become a good strategy for developing active anion transporters.<sup>[55,56,68]</sup> Last but not least, positioning the alkyl residues suitably along ion-conducting path is to some extent linked with dehydration effects of anion-binding sites<sup>[70, 73]</sup>.

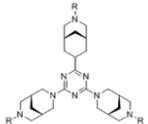
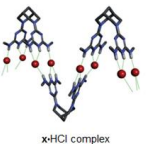
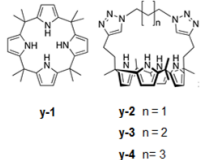
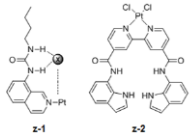
Table 1. Molecular carriers employed in effective transporters design

Carriers	Anion binding	Transport performances	Perspectives provided
<p><b>Mono(thio)urea [a] [b]</b></p>  <p>a-1-31, X=O/S</p> <p>b-1 R<sub>1</sub>=H, R<sub>2</sub>=hexyl  b-2 R<sub>1</sub>=ethyl, R<sub>2</sub>=hexyl  b-3 R<sub>1</sub>=H, R<sub>2</sub>=undecyl  b-4 R<sub>1</sub>=ethyl, R<sub>2</sub>=nonyl  b-5 R<sub>1</sub>=pentyl, R<sub>2</sub>=hexyl  b-6 R<sub>1</sub>=octyl, R<sub>2</sub>=propyl  b-7 R<sub>1</sub>=nonyl, R<sub>2</sub>=ethyl  b-8 R<sub>1</sub>=pentyl, R<sub>2</sub>=cyclohexyl</p>	<p><b>Urea or Thiourea</b></p> <p>NH...Cl<sup>-</sup> hydrogen bonds,  Compounds [d] with a polar cavity assisted by five bridged H-bonded water molecules (*MD simulations)</p>	<p>[a] Cl<sup>-</sup> transport,  <b>a-1</b> (X=S) with *EC<sub>50</sub> = 0.42mol%;  [b] Cl<sup>-</sup> transport via Cl<sup>-</sup> / NO<sub>3</sub><sup>-</sup> antiport,  <b>b-1</b> activity with EC<sub>50</sub> at 0.08mol %.</p>	<p>[a] The carriers localize within the cytoplasm of living cells<sup>[50]</sup>.  [b] Lipophilic balance as a new principle for efficient carrier design<sup>[51]</sup>.</p>
<p><b>Ortho-Phenylene bis-urea [c]</b></p>  <p>c-1 R<sub>1</sub>=R<sub>2</sub>=F  c-2 R<sub>1</sub>=R<sub>2</sub>=Cl  c-3 R<sub>1</sub>=H, R<sub>2</sub>=CF<sub>3</sub></p>		<p>[c] Cl<sup>-</sup> transport.</p>	<p>[c] Anionophore <b>c-1</b> with a difluorinated central scaffold is effective in both cells and synthetic vesicles<sup>[52]</sup>.</p>
<p><b>Benzoxazine-based tris-urea [d]</b></p>  <p>d-1-2</p>		<p>[d] Cl<sup>-</sup> transport <i>via</i> antiport exchange, compound <b>d-2</b> with EC<sub>50</sub> = 8.2 uM.</p>	<p>[d] Tris-urea compounds better carriers than tris-amide counterparts for more acidic N-H groups available<sup>[53]</sup>.</p>
<p><b>Tripodal thiourea [e]</b></p>  <p>e</p>		<p>[e] Fatty acid - activated proton transport, Compound <b>e</b> with EC<sub>50</sub> = 0.0021 mol%.</p>	<p>[e] The first example of synthetic anion receptors regulated by fatty acid<sup>[54]</sup>.</p>

<p>Fluorinated tripodal tris -thiourea [<b>f,g</b>]</p>  <p>R= </p> <p><b>f</b> <b>g</b></p>		<p>[<b>f</b>] Proton carrier or oleic acid - required Cl<sup>-</sup> transport;</p> <p>[<b>g</b>] Cl<sup>-</sup> transport <i>via</i> antiport mechanism, compound <b>g</b> with with EC<sub>50</sub> = 0.0004 mol%.</p>	<p>[<b>f</b>] Strong carrier-lipid interactions among fluorinated analogues<sup>[55]</sup>.</p> <p>[<b>g</b>] Carrier lipophilicity increases with the degree of fluorination, as the major contributing factor in transport activity<sup>[56]</sup>.</p>
<p>Bis(sulfonamide) [<b>h, i</b>]</p>  <p><b>h</b> <b>i</b></p>		<p>Cl<sup>-</sup> transport via antiport exchange,</p> <p>[<b>h</b>] EC<sub>50</sub> = 5.89 μM and *log P = 4.84;</p> <p>[<b>i</b>] EC<sub>50</sub> = 10 μM and log P = 5.84.</p>	<p>[<b>h</b>] Transport activity superior for high acidic bis-(carboxylic amide N-H)<sup>[57]</sup>.</p> <p>[<b>i</b>] pH-gated inversion of ion selectivity from cation to anion at acidic pH<sup>[58]</sup>.</p>
<p>Isophthalamide [<b>j</b>]</p>  <p><b>j-1</b> X = CH<sub>3</sub> <b>j-2</b> X = H <b>j-3</b> X = CN <b>j-4</b> X = NO<sub>2</sub> <b>j-5</b> X = H <b>j-6</b> X = NO<sub>2</sub></p>	<p>(Sulfon)amide</p> <p>NH...Cl<sup>-</sup> hydrogen-bonds, assisted by :</p>	<p>[<b>j</b>] Cl<sup>-</sup> transport</p>	<p>[<b>j</b>] The first proposed structure model to account for channel formation, that is more efficient for electron-withdrawing groups like CN and NO<sub>2</sub>.<sup>[59]</sup></p>
<p>4,6-dihydroxyisophthalamide core [<b>k</b>]</p>  <p><b>prodigiosin</b></p> <p><b>k-1</b> R = n-butyl <b>k-2</b> R = isopentyl <b>k-3</b> R = n-octyl</p>		<p>[<b>h,i</b>] CH...anion interactions, [<b>j</b>] electrostatic interactions, [<b>j</b>] π-π stacking resulting in the formation of rosette channel-pore ~8 Å diameter</p>	<p>[<b>k</b>] Cl<sup>-</sup> / HCO<sub>3</sub><sup>-</sup> exchange, transport efficiency compared with *prodigiosin.</p>
<p>Imidazole isophthalamide [<b>l</b>]</p>  <p><b>l-1</b> X = N <b>l-2</b> X = CH</p>		<p>[<b>l</b>] Either H<sup>+</sup> / Cl<sup>-</sup> symport or Cl<sup>-</sup> transport <i>via</i> an exchange mechanism.</p>	<p>[<b>l</b>] Pre-organized molecular structure exhibiting high membrane transport flux<sup>[61]</sup>.</p>

<p style="text-align: center;"><b>Squaramide [m-o]</b></p>	<p><b>Squaramide</b> Carrier, cooperative NH<math>\cdots</math>Cl<math>^-</math> H- bonding.</p>	<p>[m] Cl<math>^-</math> transport <i>via</i> an exchange mechanism; [n] Cl<math>^-</math> /NO<math>_3^-</math> exchange; [o] Cl<math>^-</math> transport by promoting NaCl influx; [m-3] glycine transport <i>via</i> OH<math>^-</math>/ H<math>_2</math>NCOO<math>^-</math> antiport.</p>	<p>[m] Squaramide functionality improves transport activities than analogous urea<sup>[62]</sup>. [n] Introduction of squaramide units in axial positions of steroidal framework confers high anion affinity/transport activity, but there exists an upper limit<sup>[63]</sup>. [o] The first experimental evidence that synthetic ion carriers can disrupt autophagy and induce apoptosis as well <sup>[64]</sup>. [m-3] New perspectives toward transmembrane delivery of cargos involving amine groups in nature<sup>[65]</sup>.</p>
<p style="text-align: center;"><b>Thiosquaramides [p]</b></p> <p style="font-size: small;"> <b>p-1</b> R<math>_1</math>=H, R<math>_2</math>=H  <b>p-2</b> R<math>_1</math>=H, R<math>_2</math>=CF<math>_3</math>  <b>p-3</b> R<math>_1</math>=CF<math>_3</math>, R<math>_2</math>=H  <b>p-4</b> R<math>_1</math>=tBu, R<math>_2</math>=H </p>		<p>[p] Cl<math>^-</math> transport <i>via</i> Cl<math>^-</math>/NO<math>_3^-</math> exchange, regulated by pH, efficient transporter activated at pH 4 with EC<math>_{50}</math> = 0.0125 mol%.</p>	<p>[p] One of the few synthetic ionophores with truly controllable anion transport switch<sup>[66]</sup>.</p>
<p style="text-align: center;"><b>Oxothiosquaramide [q]</b></p> <p style="font-size: small; text-align: center;">q-[1-2]</p>		<p>[q] Cl<math>^-</math> transport <i>via</i> antiport mechanism, regulated by pH, efficient transporter activated at pH 4 with EC<math>_{50}</math> = 0.03 mol%</p>	<p>[q] Adding sulfur motifs to the squaramide structure induces a controlled pH switch<sup>[67]</sup>.</p>
<p style="text-align: center;"><b>Indole-based [r]</b></p>		<p><b>Indole</b> Carrier, [r,t] cooperative NH<math>\cdots</math>Cl<math>^-</math> H- bonds <i>via</i> indole, (thio)urea</p>	<p>[r] Cl<math>^-</math> transport <i>via</i> Cl<math>^-</math>/NO<math>_3^-</math> or Cl<math>^-</math>/HCO<math>_3^-</math> antiport or HCl symport, compound <b>r-4</b> with efficiency EC<math>_{50}</math> = 0.005mol% and log P = 6.40.</p>

 <p>r-1 X = O, R<sub>1</sub> = H, R<sub>2</sub> = H  r-2 X = S, R<sub>1</sub> = H, R<sub>2</sub> = H  r-3 X = O, R<sub>1</sub> = CF<sub>3</sub>, R<sub>2</sub> = <sup>t</sup>Bu  r-4 X = S, R<sub>1</sub> = CF<sub>3</sub>, R<sub>2</sub> = <sup>t</sup>Bu</p>	<p>or pyrrole groups,  [s] NH...F<sup>-</sup> H-bonds, F<sup>-</sup>  bound in a twisted  conformation.</p>		
<p>Indole-functionalized isophthalamides [s]</p>  <p>s-1 X = N  s-2 X = CH</p>		<p>[s] F<sup>-</sup> recognition, fluoride complex almost  3-fold more stable than chloride binding<sup>[69]</sup>.</p>	/
<p>Indole-based perenosins [t]</p>  <p>t-1 R<sub>1</sub> = Me, R<sub>2</sub> = Pent, R<sub>3</sub> = H  t-2 R<sub>1</sub> = CF<sub>3</sub>, R<sub>2</sub> = Pent, R<sub>3</sub> = H  t-3 R<sub>1</sub> = Me, R<sub>2</sub> = Prop, R<sub>3</sub> = H  t-4 R<sub>1</sub> = Me, R<sub>2</sub> = H, R<sub>3</sub> = Pent  t-5 R<sub>1</sub> = Me, R<sub>2</sub> = Pent, R<sub>3</sub> = Pent</p>		<p>[t] Inseparable HCl symport, compound <b>t-3</b>  with efficiency EC<sub>50</sub> = 0.00069 mol%.</p>	<p>[t] Identical substituents on different positions  of perenosin backbone significantly alters  transport properties due to different  encapsulation effects<sup>[70]</sup>.</p>
<p>Phenylthiosemicarbazones [u]</p>  <p>u-1 R = H  u-2 R = OCH<sub>3</sub>  u-3 R = CF<sub>3</sub></p>	<p><b>Semicarbazones</b>  H-bonding.</p>	<p>[u] Inseparable H<sup>+</sup>/Cl<sup>-</sup> cotransport regulated  by pH, compound <b>u-1</b> with  EC<sub>50</sub>(pH:7.2)/EC<sub>50</sub>(pH:4.0) = 660.</p>	<p>[u] The first pH-switchable non-electrogenic  anion transporter that truly mimics  prodigiosin's transport behaviors<sup>[71]</sup>.</p>
<p>Tambjamine derivatives [v]</p>  <p>v series</p>	<p><b>Tambjamine</b><sup>[72]</sup>  NH...Cl<sup>-</sup> H-bonds.</p>	<p>[v] Cl<sup>-</sup> transport,  EC<sub>50</sub> = 0.00312 mol%.</p>	<p>[v] Quantitative lipophilicity as a  contributing factor in transport activity of  tambjamine analogues<sup>[73]</sup>.</p>

<p>Tripodal triazines [w]</p>  <p>w-1 R = CH<sub>2</sub>C<sub>6</sub>H<sub>5</sub> w-2 R = CH<sub>2</sub>C<sub>6</sub>F<sub>5</sub> w-3 R = H</p>	<p><b>Bispidine</b></p> <p>Carrier with preorganized cavity, direct and water-mediated H-bonds as well as electrostatic interaction.</p>	<p>[w] Cl<sup>-</sup> transport <i>via</i> antiport exchange, compound <b>w-1</b> with EC<sub>50</sub> = 0.25 μM and log P at 7.44.</p>	<p>[w] High degree of preorganization contributes to anion recognition and transport activity<sup>[74]</sup>.</p>
<p>Bis(melamine)-Substituted Bispidine [x]</p>  <p>x·HCl complex</p> <p><i>Adapted with permission from ref. 75. Copyright 2017, Wiley-VCH.</i></p>	<p>Carrier, HCl-bound V-shaped complex as x·(HCl)<sub>2</sub> arranged in a zig-zag network, via electrostatic interactions and H-bonding.</p>	<p>[x] pH-dependent, HCl symport, maximal activity at pH=7 with EC<sub>50</sub> = 30.1 nM.</p>	<p>[x] Function in a fashion similar to that of natural anticancer agent prodigiosin<sup>[75]</sup>.</p>
<p>Calix[4]pyrrole [y]</p>  <p>y-1      y-2 n = 1 y-3 n = 2 y-4 n = 3</p>	<p><b>Calix[4]pyrrole</b></p> <p>NH...F- H-bonds.</p>	<p>[y] F<sup>-</sup> transport, with F<sup>-</sup>/Cl<sup>-</sup> selectivity at 1.8.</p>	<p>[y] The first example of small molecule carrier facilitating fluoride transport<sup>[76]</sup>.</p>
<p>Metal-organic anion receptor [z]</p>  <p>z-1      z-2</p>	<p><b>Metal-organic anion receptor</b></p> <p>H-bonding and [z-2] electrostatic interaction.</p>	<p>[z-1] SO<sub>4</sub><sup>2-</sup> binding<sup>[77]</sup>; [z-2] H<sub>2</sub>PO<sub>4</sub><sup>-</sup> selectivity.</p>	<p>[z-2] The first example of metal-induced pre-organization to enhance anion affinity in a neutral receptor<sup>[78]</sup>.</p>

\* MDS, molecular dynamic simulation.

\* EC<sub>50</sub>, transporter needed to obtain 50% ion transport activity expressed either in molar concentration or in mol% of carrier with respect to lipid.

\* log P, lipophilicity, i.e., partition coefficient in octanol-water.

\* Prodigiosin, a natural product best known as a nonelectrogenic transporter that facilitates H<sup>+</sup>/Cl<sup>-</sup> cotransport<sup>[79]</sup>.

**Self-assembled anion-channels.** In natural channels, the alignment of binding sites pointing toward a central pore is used to combine selectivity *via* precise bonding in the selectivity filters with high speed multi-ion hopping translocation along pore-aligned recognition sites. To achieve further significant transmembrane transport, it is essential to construct anion-channels aligning multiple binding sites, as mostly demonstrated within cation-channels. There exist different strategies when it comes to supramolecular channel fabrication. Unimolecular, micellar, barrel-stave, barrel-hoop, barrel-rosette or metal-organic cages self-assembled channels have been described.<sup>[81]</sup> Supramolecular self-assembled barrel rosette-type channels with a sufficient length for spanning the lipid bilayer membrane and appropriate anion binding cavities for the transport have been mostly reported.

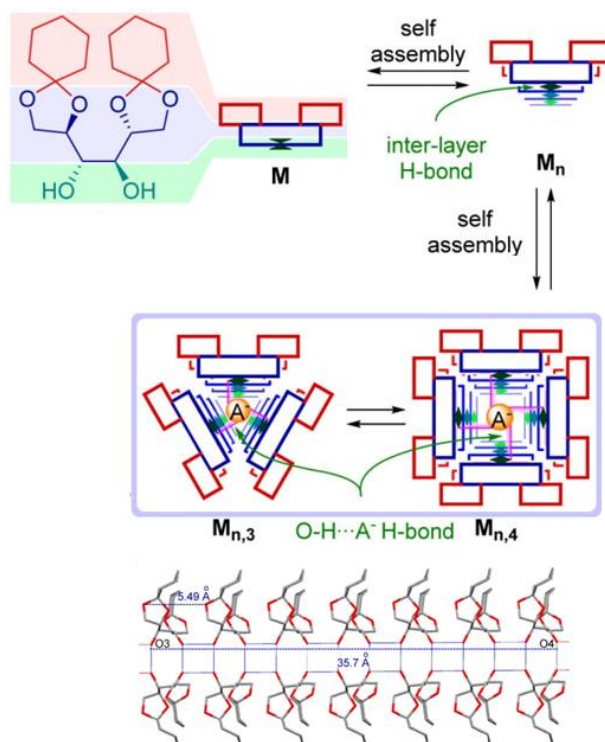


**Figure 23.** Chemical structure of diketal-protected mannitol (**M**) and its ladder-like crystal structure with single-file anion recognition sites. Inter-layer self-assembly and anion-induced formation of hydrogen-bonding rosette-type channels. Adapted with permission from ref. 47b. Copyright 2014, American Chemical Society.



Talukdar group have constructed various self-assembled channels to transport anions across lipid bilayer membranes. In 2014, they reported diketal-protected mannitols (**M**s) able to form rosette-type ion channels *via* multiple intermolecular hydrogen-bonding in bilayer membrane.<sup>[47]</sup> Nanotubular structures in solid state supported their hypothesis of a translocation single-file relay mechanism for  $\text{Cl}^-$  jumping from one binding site to the next *via* multivalent  $\text{OH}\cdots\text{Cl}^-$  H-bond interactions (Figure 23). Distinct single-channel currents were recorded and the formed supramolecular rosette-type channels exhibited ohmic, anion selective transport ability.

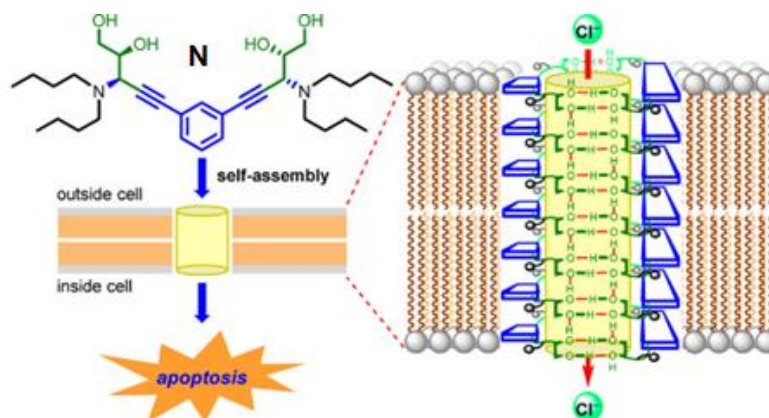


**Figure 24.** Self-assembly of chiral ethylene glycol **N** into barrel rosette-type chloride anion channels in lipid bilayer membranes. Adapted with permission from ref. 82 Copyright 2016, American Chemical Society.

Shortly, the same group reported that chiral ethylene glycol **N** with four hydrophobic alkyl tail could self-assemble into supramolecular rosette ion channels in lipid bilayer membrane with highly selective transport of chloride ions via an  $\text{OH}^-/\text{A}^-$  antiport mechanism (Figure 24).<sup>[82]</sup> Based on theoretical calculation, the authors proposed a barrel-rosette ion channel formation through intermolecular hydrogen-bonding between hydroxyl groups. In addition, these channels can induce apoptosis via transmembrane transport of chloride ions through living cells.

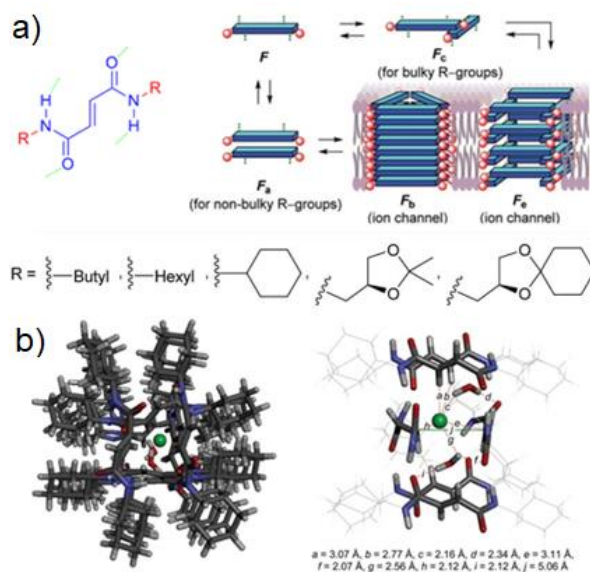


**Figure 25.** a) Self-assembly of fumaramide derivatives and b) geometry optimized H<sub>2</sub>O-mediated Cl<sup>-</sup> binding channel model. Adapted with permission from ref. 83. Copyright 2018, The Royal Society of Chemistry.

Functionalized fumaramides were found to self-assemble into transmembrane anion channels in lipid bilayer membrane.<sup>[83]</sup> For example, if fumaramide is equipped with non-bulky terminal R-groups readily assembles through intermolecular C=O...H-N H-bonds as a flat-ribbon-shaped unit (**F<sub>a</sub>**) which subsequently stacks to form a higher-ordered and exceptionally stable nanotubular architecture (**F<sub>b</sub>**). Meantime, the introduction of bulky cyclohexyl substituents affords an orthogonally oriented dimer (**F<sub>c</sub>**), favoring the formation of an active rosette-type channel (**F<sub>e</sub>**) (Figure 25a). Such an assembled channel displayed selective transport for Cl<sup>-</sup> anions, with EC<sub>50</sub> = 3.5 μM and a good Cl<sup>-</sup> *versus* K<sup>+</sup> selectivity of S<sub>Cl<sup>-</sup>/K<sup>+</sup></sub> = 28.5). According to an optimized hydrated channel model based on the known crystal structure, the driving force for Cl<sup>-</sup> flux is a combination of anion-π interaction with the electron-deficient alkene moieties, C-H...anion interactions as well as Cl<sup>-</sup> hydrogen-bonding with the lubricant water molecules bound to the fumaramide carbonyl groups (Figure 25b).

Amphiphilic heptapeptides<sup>[84]</sup>  $(R^1)_2\text{NCOCH}_2\text{OCH}_2\text{CO}-(\text{Gly})_3\text{Pro}(\text{Gly})_3-\text{OR}^2$  is a classic type of synthetic peptide designed and tested by Gokel et al. as  $\text{Cl}^-$ -selective self-assembled channels. They've found that structural variations on side-chains or termini of the peptide residues and even the phospholipid composition would exert influences toward  $\text{Cl}^-$  release efficiency from liposomes. Through NMR titration studies as well as MD simulation, they achieved the structural analysis of peptide-based channel, in which peptide residues would interact with the salt as an ion pair and H-bond to  $\text{Cl}^-$  anion<sup>[85]</sup>.

More recently, Talukdar et al. discovered the importance of fluorination of the peptide backbones for its aggregation<sup>[86]</sup>. They reported that tripeptides with fluorine substituents present a reverse-turn U-shaped conformation, whereas the non-fluorinated counterparts only displayed disordered states. This difference was attributed to the cooperative effects between intramolecular hydrogen-bonding ( $\text{HN}\cdots\text{F}\cdots\text{HN}$ , 2.091 Å and 2.206 Å, by DFT calculations) and  $\text{N}^+\cdots\text{F}^{\delta-}$  charge-dipole attraction (Figure 26). Such a U-shaped monomer further aggregated into extended antiparallel helical stacks, with selective  $\text{Cl}^-$  transport efficiency  $\text{EC}_{50}=15.83 \text{ uM}$ .

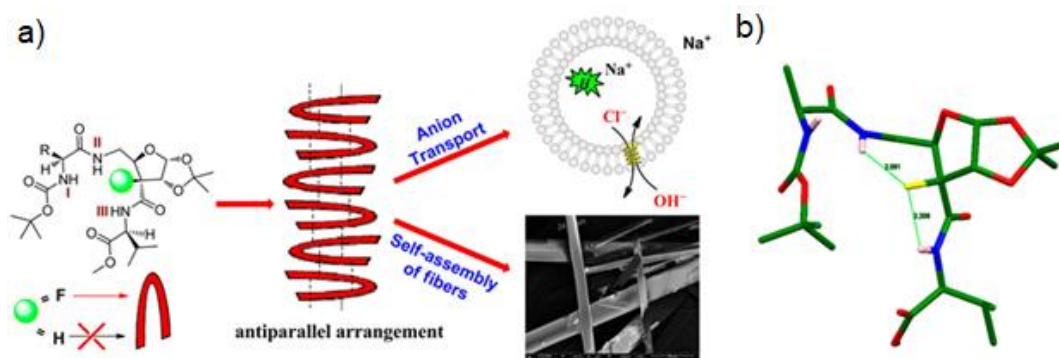


**Figure 26.** a) Fluorination-induced reverse-turn self-assembly and transmembrane ion transport within EYPC-vesicles; b) molecular structure of the tripeptide with minimum energy calculated from DFT ( $\text{R} = -\text{CH}_3$ ). Adapted with permission from ref. 86. Copyright 2017, American Chemical Society.

Zeng et al. developed peptide-backbones as anion-active artificial channels, self-assembled *via* hydrogen-bonding, van der Waals interactions and stacking interactions. They have screened a combinational library of 100 compounds and experimentally and theoretically identified highly functional channel-forming channel-type superstructures in bilayer membrane. They found a unique directional rod-like hydrogen-bonding self-assembled superstructure of **Fmoc-Phe-C4** as an exceptionally active anion channel **6L10**,  $EC_{50} = 0.05$  mol % relative to lipid for nitrate anions (Figure 27a).<sup>[87]</sup> Consequently, they presented an extended tripeptide **6L310** with stable pore-forming ability and reported an impressive nanomolar range activity for the anions transport with  $EC_{50} = 0.005$ – $0.013$  mol % relative to lipid (Figure 27b).<sup>[88]</sup>

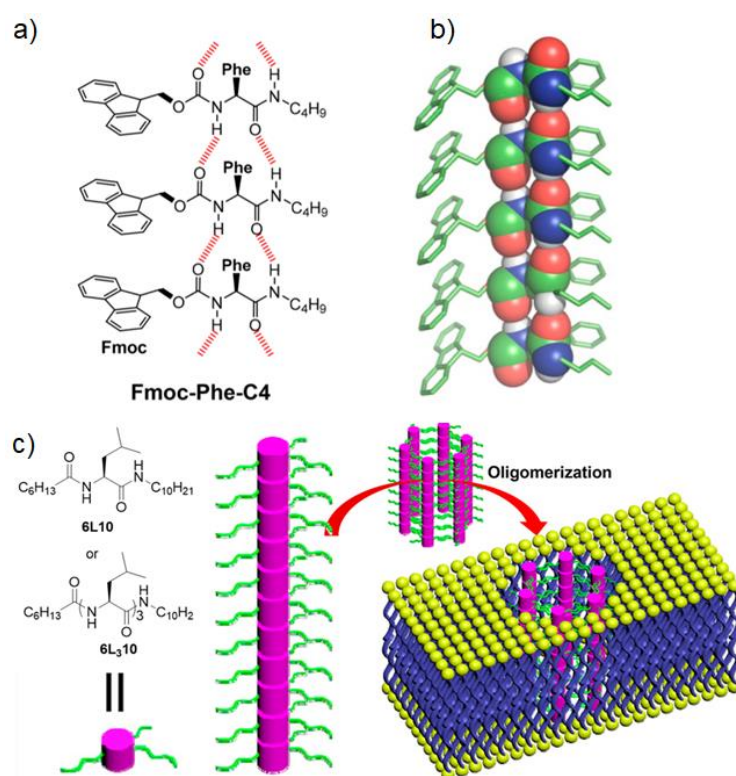


**Figure 27.** A) Chemical structure and B) single crystal structures of model compound **Fmoc-Phe-C4**, and C), chemical structures of **6L10** and **6L310** and their self-assembly into hexameric tubular channels for anion transport. *Adapted with permission from ref.87. Copyright 2018-2019, American Chemical Society.*

In 2007, Yang et al. designed a lipophilic dipeptide-based molecule **Yang-1** with four amide groups, readily assembling into a channel-superstructures for Cl<sup>-</sup> translocation, as confirmed by single-channel current activity detected with planar patch-clamp experiments (Figure 28)<sup>[89]</sup>. Later it was found that this supramolecular architecture is also able to promote Cl<sup>-</sup> transport in living human cystic fibrosis epithelial cells<sup>[90]</sup>, and as the first example, to regulate natural voltage-gated Ca<sup>2+</sup> channels restoring the membrane potential equilibrium through increasing Cl<sup>-</sup> membrane permeability<sup>[91]</sup>. In light of these findings, this study sets a good example on rationally designed functional artificial channels assembled from very simple and small molecules.

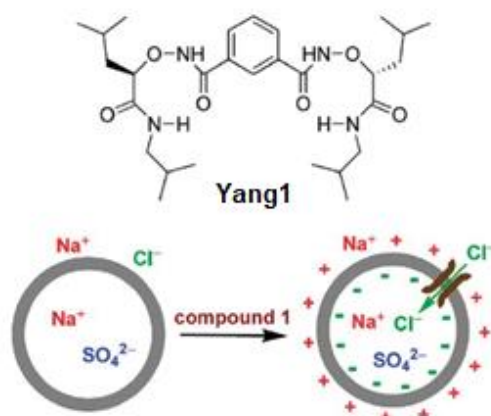


**Figure 28.** Self-assembled rosette-channels **Yang -1** as chloride regulator within vesicles. Adapted with permission from ref.89. Copyright 2007, American Chemical Society.

Halogen bonds<sup>[92]</sup> have recently been introduced as ideal scaffolds to transport anions across lipid bilayer membranes. Matile group pioneered this field and firstly used the halogen<sup>[93]</sup> and chalcogen and pnictogen bonds<sup>[94]</sup> to transport Cl<sup>-</sup>/anions by employing small molecules, but the obtained transport activities were not impressive. In the meantime, they designed linear channel-oriented molecules, which can linearly align as rigid-rod scaffolds for anion hopping along transmembrane channels with excellent activities and an unprecedented cooperativity coefficient  $m = 3.37$  (Figure 29).<sup>[95]</sup>

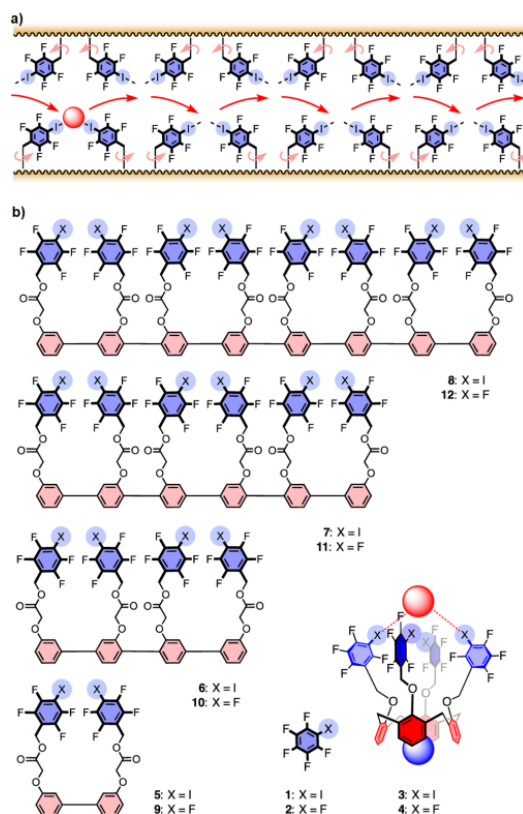


**Figure 29.** a) Schematic representation of anion hopping along transmembrane halogen-bonding cascades. b) Halogen-bond donors as channels and carriers *Adapted with permission from ref. 95. Copyright 2013, American Chemical Society.*

Later, Zeng et al. used functionalized tetrafluoroiodobenzyl peptide scaffolds as multiple recognition sites for  $\text{Cl}^-$  transport through halogen bonding. After screening 15 peptides, three Ala/Leu-based compounds (**A10**, **L8** and **L10**) were identified to be very active as anion channels in lipid bilayer.<sup>[96]</sup> MD simulations showed that 6-7 molecules of peptide **L8** self-assemble *via* the intermolecular hydrogen-bonding to align the iodine atoms as halogen bond donors along as a single-file chain. The authors reported that such halogen bond-mediated artificial channels exhibited superior  $\text{Cl}^-$  transport activity over other previously reported halogen bond-based active carriers and channels. Importantly, the synthetic artificial ion channel **A10** presented a high anticancer activity: excellent  $\text{IC}_{50} = 20 \mu\text{M}$  against human breast cells (BT-474), even superior to well-known anticancer agent cisplatin under identical conditions.



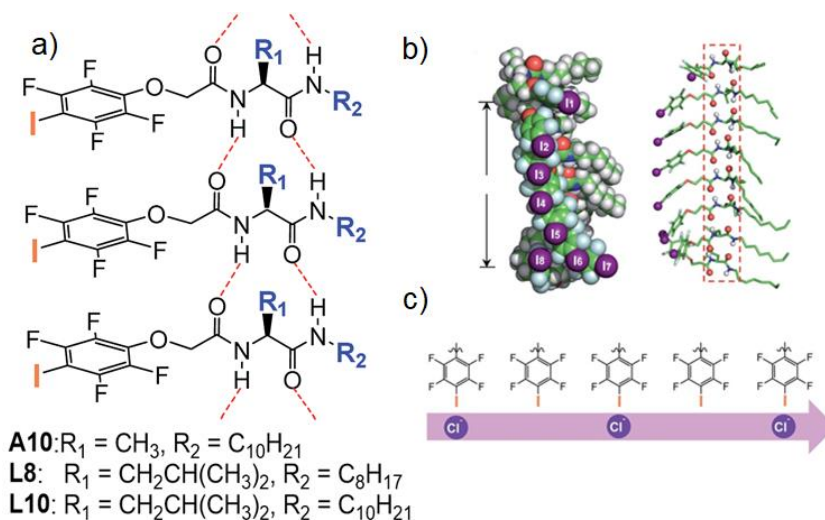


**Figure 30.** a) Tetrafluoriodobenzyl-peptides **A10**, **L8** and **L10** as  $\text{Cl}^-$ - recognition/translocation channels; b) theoretical structure for **L8** and c)  $\text{Cl}^-$ - single file array. *Adapted with permission from ref. 96. Copyright 2018, Royal Society of Chemistry.*

Anion translocation along multi-ion hopping directional pathways have been also observed in channel architectures constructed with anion- $\pi$  slides.<sup>[97-101]</sup> The anion- $\pi$  interactions, not known in biological channels, has been extensively used for anion encapsulation and recognition.<sup>[102-105]</sup> The possibility to create synergetic selective translocation functions with anion channels is therefore attractive and inspiring.

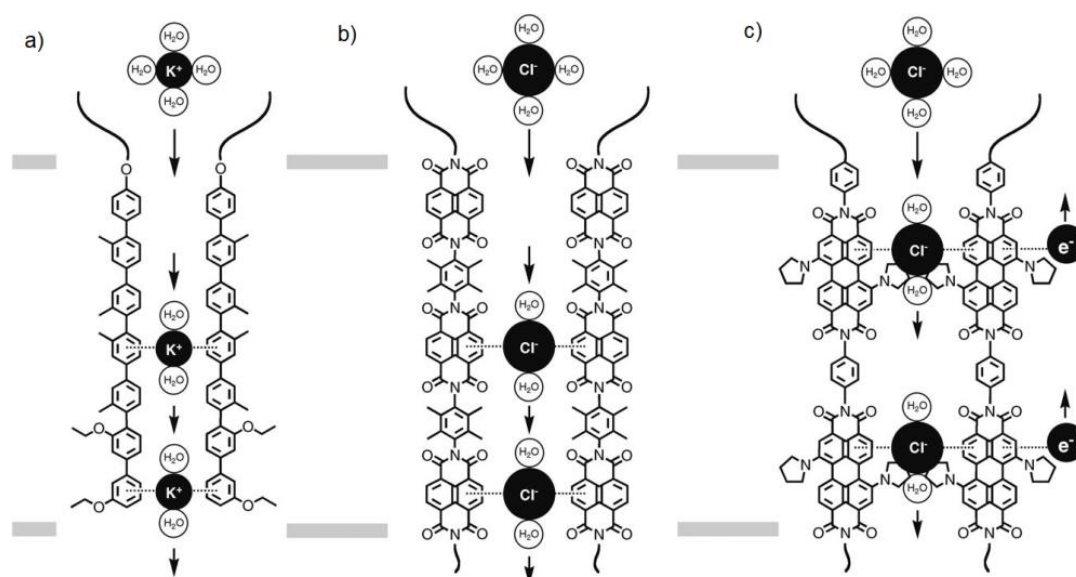


**Figure 31.** Structures of a) Rigid p-oligophenyl cation- $\pi$ ; b) oligonaphthalenedimide and c) oligoperylene-dimide anion- $\pi$  slides. *Adapted with permission from ref. 101. Copyright 2009, Wiley WCH.*

---

Rigid  $\pi$ -basic p-oligophenyl rigid-rods have been explored as cation- $\pi$  slides to achieve transmembrane  $K^+$  transport with cation- $\pi$  interactions (Figure 31a). Moreover, the  $\pi$ -acidic oligonaphthalenediimides (O-NDIs) (Figure 31b) or oligoperylenediimides (O-PDIs) (Figure 31c) have been introduced by Matile et al. to translocate anions *via* anion- $\pi$  slides.<sup>[101]</sup> The halide selectivity sequence  $Cl^- \sim F^- > Br^- > I^-$  has been experimentally reported, reminiscent with the partial anion dehydration, fully compensated by strong anion binding to rigid slide-rods of (O-NDIs).<sup>[97]</sup>

So far, the combination of anion recognition *via* hydrogen-bonding, ion-pairing and anion-dipole interaction featured by selective anion-carrier systems with anion- $\pi$  oriented translocation featured by anion- $\pi$  slides channels, can be synergistically employed to synergistically promote selectivity while maintaining a reasonable high transport rate, as observed for transmembrane natural channels. Recently, Barboiu et al. reported a class of supramolecular channels self-assembled by triazole amphiphiles<sup>[106]</sup>. Single-crystal structures reveal the self-assembly of  $TC4H^+ \cdot X^-$  ( $Cl^-$ ,  $Br^-$ ,  $I^-$ ,  $NO_3^-$ ) in columnar architectures of stacked protonated triazole quartets-T4, stabilized by multiple hydrogen-bonding, anion- $\pi$  and aromatic stacking interactions with anions. In bilayer membranes, low transport activity was observed when the T4-channels were operated as  $H^+/X^-$  translocators, but higher transport activity was observed for  $X^-$  in the presence of the  $K^+$ -carrier valinomycin. These self-assembled superstructures, presenting intriguing structural behaviors such as directionality and strong anion encapsulation by hydrogen-bonding supported by vicinal anion- $\pi$  interactions, can serve as artificial supramolecular channels for transporting anions across lipid bilayer membranes.



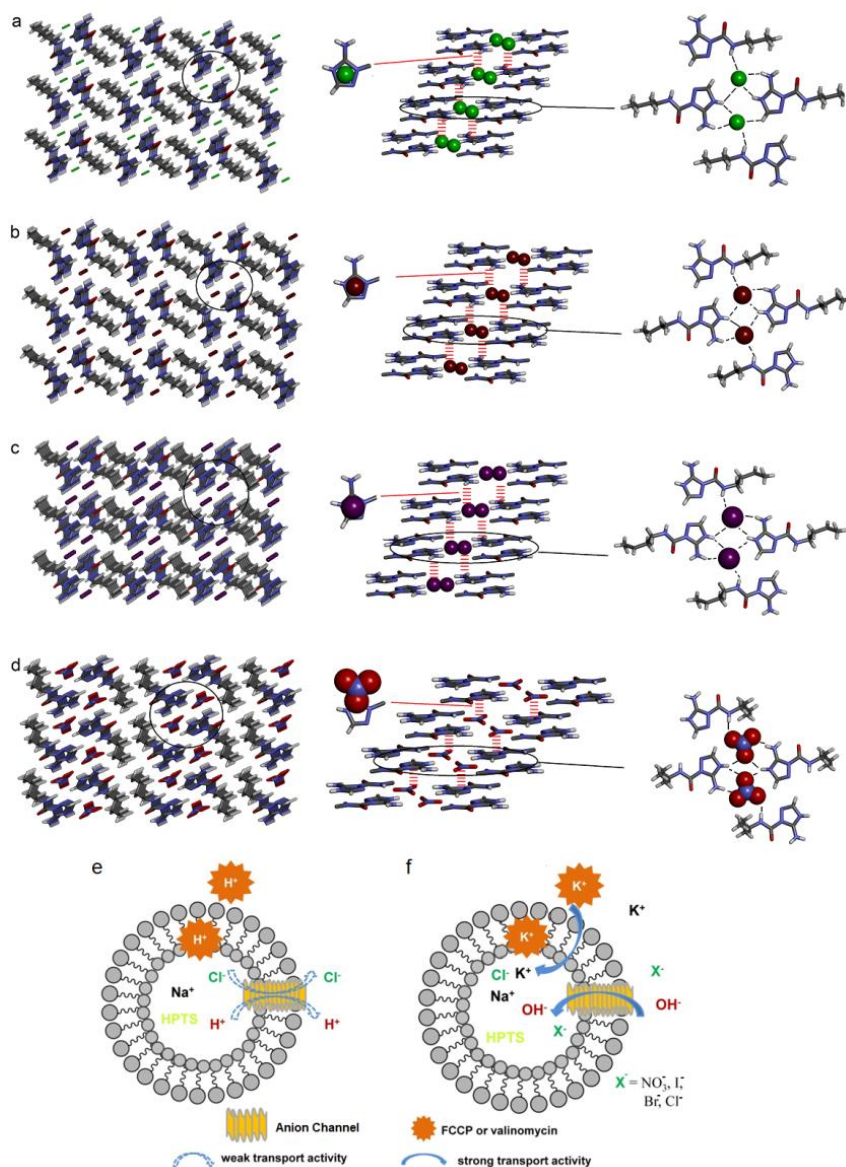


**Figure 1.** X-ray crystal structures of  $\text{TH}^+\text{C}_4 \cdot \text{X}^-$ ,  $\text{X}^- =$  a)  $\text{Cl}^-$ , b)  $\text{Br}^-$ , c)  $\text{I}^-$  and d)  $\text{NO}_3^-$ . crystal packing revealing the formation of the anion-channels of T quartets presenting anion- $\pi$  interactions (red lines). Proposed transport mechanism of  $\text{TH}^+\text{C}_{12} \cdot \text{Cl}^-$  in the presence of e) FCCP as  $\text{H}^+$  carrier or f) valinomycin as a  $\text{K}^+$  carrier

**Metal organic cages/polyhedra-based anion channels.** Previous investigations have demonstrated specific membrane insertion behaviors and selective ionic transport when nanocapsules have been used as selective pore for cation translocation.<sup>[40-46]</sup> Importantly, the nanocapsule functionalities like pore aperture, internal surface properties or grafted recognition groups have the potential to be widely tuned in order to control properties such as selectivity for the ion flux.

In 2017, Kim et al. introduced a porous organic porphyrin box presenting a large internal cavity, porosity and appropriate length to fit the thickness of a lipid bilayer membrane as iodide-selective channels.<sup>[107]</sup> The porphyrin box-channel with octyloxy-side groups rendered a specific transport preference for  $\text{I}^-$  anions over the other anions in lipid bilayer membrane, favored by their lowest dehydration energy. Long-lived current profiles with open and closed states confirmed the channel transport mechanism for  $\text{I}^-$  anions. The channels are able to transport  $\text{I}^-$  anion through membranes of living cells, indicating their potential application in clinical treatment for iodide associated diseases.

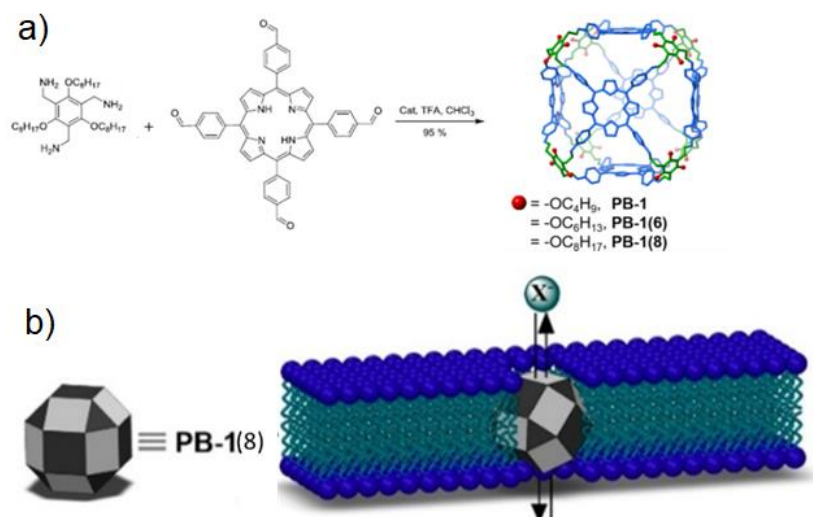


**Figure 33.** a) Synthesis of metal organic cages **PB-1**, **PB-1(6)** and **PB-1(8)** from lipophilic trisamine and tetraporphyrinaldehyde *via* amine/aldehyde imine chemistry; b) schematic diagram for transport of **PB-1(8)** towards anions in lipid bilayer membrane. *Adapted with permission from ref.107. Copyright 2017, American Chemical Society.*

Keyser et al.<sup>[108a]</sup> functionalized with long alkyl chain ( $\text{C}_9\text{H}_{19}$ ) a previously reported pentagonal prism  $\text{Zn}_{10}\text{L}_{15}$  prepared by Nitschke group<sup>[108b]</sup> from iminobispyridine ligands and metal salts *via* subcomponent self-assembly (Figure 34a). They found that the pentagonal prismatic architecture with a central channel-like cavity at diameter 2.3 Å preferred to bind a halide anion within the pocket and form lockable long-lived, ohmic,

Cl<sup>-</sup> channels in lipid bilayer membranes. Notably, these anion channels can be blocked by addition of sodium dodecyl sulfate (Figure 34b).

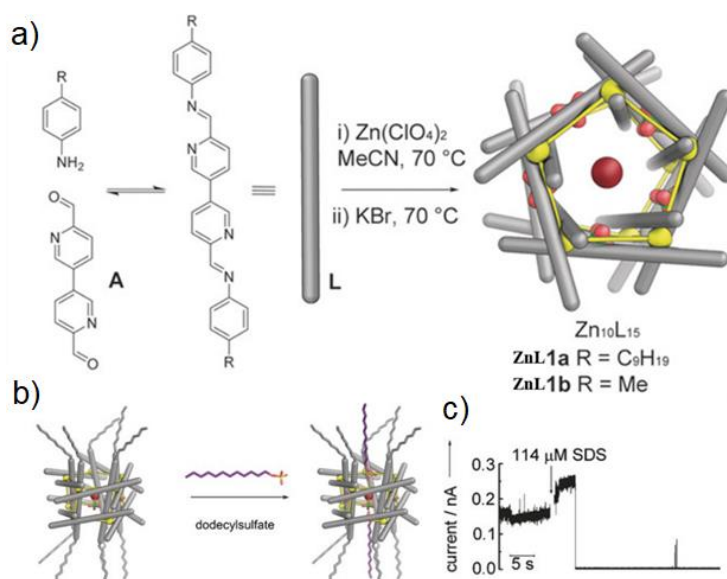


**Figure 34.** a) Synthesis of pentagonal prisms **ZnL1a** and **ZnL1b** for the halide ion recognition; b) the dodecyl sulfate "switch off" mechanism of the active channel **ZnL1a**, and (c) typical "switching off" current trace of **ZnL1a**. Adapted with permission from ref.108a. Copyright 2017, Wiley VCH.

#### 4. Applications of supramolecular artificial channels

Supramolecular artificial channels have found uses in a variety of fields, some in physiology and chemistry. The not exclusive examples presented in these paper (Table 2), let us imagine that high activity of natural channels can be obtained by using simpler artificial self-assembled channels displaying selectivity functions *like the natural ones*. The future may involve all-made *artificial biomimetic channels* by using synthetic approaches. All examples presented here would also do much to restore some balance to our understanding of the biomimicking of functions of natural proteins and remains an important exploring applicative challenge. The channel systems provide remarkable combinations of applications in materials sciences (sensing, photosystems), biology (cellular uptake), and medicine, very close to those encountered in natural systems.

**Table 2.** A summary of selected masterpiece of artificial channels, comparison to natural channels and biological activity

Compound	Nature of the channel	Selectivity/ permeability, single channel ion flux, etc	Comparison to natural channel	Reference Figure
<b>5F8</b>	Directional inherent hydrophilic cavity by intermolecular multiple H-bonds	K <sup>+</sup> conduction rate $\gamma_{K^+} = 26.4 \pm 2.8$ pS and $S_{K^+/Na^+} = 9.8$	K <sup>+</sup> conduction rate ( $\gamma_{K^+} = 26.4 \pm 2.8$ pS) close to that of Gramicidin A ( $\gamma_{K^+} = 23.2 \pm 0.4$ pS).	[12] Figure 3
<b>CP1</b>	Hydrophilic cyclopeptide nanotubes self-assembled <i>via</i> a) intermolecular peptide bonds H-bonding and b) hydrophobic interactions between side chains.	K <sup>+</sup> flux of $2.2 \cdot 10^7$ ions s <sup>-1</sup>	Three times faster than gramicidin A.	[20a] Figure 9
<b>4</b>	Hydrophobic tubular channel (6.4 Å) via $\pi$ - $\pi$ stacking of arylene-ethynylenes macrocycles and H-bonding of side dipeptides	1) selectivity $S_{H^+/Cl^-} = 3,000$ 2) Pemeability, $P = 4.9 \cdot 10^7$ water molecules/s/ channel	a) H <sup>+</sup> selectivity higher than that of natural influenza M2 proton channels ( $P_{H^+}/P_{Cl^-} = 19.7$ ) b) 22% permeability of natural water channel AQP1	[25] Figure 10c
<b>g1d and g1e</b>	Hydrophilic tubular channels driven by a) the intramolecular hydrogen bonding and b) layer-by-layer aromatic stacking interactions	High conductance towards K <sup>+</sup> ions, up to $770 \pm 30$ and $890 \pm 52$ pS (0.5 M KCl)	Comparable to that of natural protein toxin, $\alpha$ -hemolysin (800 to 1000 pS) under similar conditions.	[23]
<b>A2, A4, A5</b>	Hydrophilic helical channel (1.0 nm) via intramolecular hydrogen bonding in aromatic hydrazide foldamers	exceptionally high NH <sub>4</sub> <sup>+</sup> /K <sup>+</sup> selectivity	1) <b>A4, A5</b> Selectivity $S_{NH_4^+/K^+} = 6$ higher than that of gramicidin A; 2) the efficiency of <b>A2</b> transport of Tl <sup>+</sup> is comparable to gramicidin A.	[28]
<b>Heptapeptide</b> or SCMTR (R <sup>1</sup> ) <sub>2</sub> NCOCH <sub>2</sub> O CH <sub>2</sub> CO- (Gly) <sub>3</sub> Pro(Gly) <sub>3</sub> -OR <sup>2</sup>	Central proline flanked with glycine residues as Cl <sup>-</sup> -binding unit and membrane anchor, two molecules assembly in the external leaflet of the bilayer resulting a pore of $\sim 6-7$ Å, voltage gating.	Cl <sup>-</sup> /K <sup>+</sup> selectivity over 10	Incorporated structural patterns from CIC family of chloride protein channels; as cellular volume modulator in mammalian cells.	[84a]
<b>Hydraphiles</b>	Diaza-18-crown-6 macrocycles as amphiphilic	Selectivity Na <sup>+</sup> over K <sup>+</sup>	Topologically similar to KcsA channel; 25-30%	[6d]

	head groups connected by 12-carbon chains as hydrophobic spacers, with overall distance $\sim 40 \text{ \AA}$ .		transport rate of gramicidin; toxicity toward bacteria, yeast and mammalian cells, and as biologically acute toxins in the muscle tissue of living mice.	Figure 1
<b>Yang1</b>	Constructed by $\alpha$ -aminoxy acid derivatives with more acidic NH units than regular amide groups.	$\text{Cl}^-$ association constant $K > 100000 \text{ M}^{-1}$	$\text{Cl}^-$ permeability in living human cystic fibrosis epithelial cell; the first synthetic ion channel able to regulate natural voltage-gated calcium channels.	[89-91] Figure 28
Monothiourea	Carrier	$\text{Cl}^-$ transport, with $\text{EC}_{50}$ at 0.42mol%	Synthetic carriers actually working within the cytoplasm of living cells.	[50]
Ortho-Phenylene bis-urea	Carrier	$\text{Cl}^-$ transport	Anionophore with a difluorinated central scaffold more effective in both cells and synthetic vesicles.	[52]
Squaramide	Carrier	$\text{Na}^+/\text{Cl}^-$ cotransport	Firstly proving synthetic ion carriers able to disrupt autophagy and induce apoptosis.	[64]
Phenylthiosemi carbazones	Carrier	$\text{H}^+/\text{Cl}^-$ cotransport regulated by pH with selectivity $\text{EC}_{50(\text{pH}:7.2)}/\text{EC}_{50(\text{pH}:4.0)}$ at 660	The first pH-gated nonelectrogenic anion transporter mimicking natural prodigiosin.	[71]
Bis(melamine)-Substituted Bispidine	Carrier	pH-gated $\text{HCl}$ symport, maximal activity at $\text{pH}=7$ with $\text{EC}_{50}$ at 30.1 nM	Functioning in a fashion similar to that of natural anticancer agent prodigiosin.	[74]
<b>L8</b>	Halogen bond-mediated anion transport based on a mono-peptide columnar H-bonded scaffold	$\text{Cl}^-$ transport with $\text{EC}_{50}$ at 0.39 $\mu\text{M}$	Potential as anticancer drug with $\text{IC}_{50}$ toward human breast cancer cell at 20 $\mu\text{M}$ .	[96] Figure 30
<b>PB-1A</b> -based channel	3D shape-persistent porphyrin cage with a cavity at $\sim 1.95 \text{ nm}$ , 12 windows at $\sim 3.7 \text{ \AA}$ and outer maximum diameter at 3.64 nm.	$\text{I}^-/\text{Cl}^-$ selectivity over 60	Actually, promoting iodide permeability through living cell membranes, with potential clinical treatment for iodide deficiency-related diseases.	[107] Figure 33
<b>Pseudopeptidic cage</b>	Carrier	pH-gated $\text{H}^+/\text{Cl}^-$ symport with chloride efflux rate $k = 0.151 \text{ Cl}^- \cdot \text{s}^{-1}$ .	Selective killing cancer cells in acidic microenvironments.	[109]

---

## Outlook and perspectives

Nature spent millions of years to build highly selective ion-channels. We had several decades to *compete* the natural channel systems and the field has been extensively developed. Yet, the aforementioned non-exclusive examples have demonstrated the promise of developing artificial channels with high selectivity and transport efficiency close to natural ones. One could say that further discovery of novel synthetic systems able to form channels is highly important. But even if the discovery is empirical, the natural proteins may serve us to tailor the functions of the synthetic systems and engineer optimized supramolecular constructs. This interdependence makes our next challenge still more ambitious: understanding the natural systems transport mechanism is often one way to raise artificial systems to the level of natural functions or even beyond.<sup>[110]</sup>

The big question here is to detect the optimal arrangement of the ion-binding sites disposed in an optimal configuration for ion translocation. Too strong ion-binding needed for selectivity, mostly described with carriers (Table 1), will slow down the ion-hopping and the fast permeability of the ion channels. The solution to this problem is to detect the optimal architectures that can balance the selectivity-permeability paradigm. Nowadays, important industrial separative processes (i.e. ion-exchange, membrane, chromatography, etc.), mostly require high selectivity and a reasonable permeability for real applications. Some systems have showed superior properties over natural channels, such as higher selectivity or ion flux. Examples include self-assembly of simple organic amphiphiles, crown-ethers, rigid rod molecules, rotaxanes, quadruplex systems, etc. (Table 2). Despite most of the artificial ion channels are lie in the porotype status, far from the channel-replacement therapy, their medical

---

applications seems to be promising. For example, Gokel et al. have proved that the supramolecular artificial channels have the enhanced antibiotic potency against *E. coli*. Zeng et al. have showed that such channel has very high anticancer activity: excellent IC<sub>50</sub> value of 20 μM against human breast cells (BT-474), even superior over well-known anticancer agent cisplatin under identical conditions. Talukdar et al supramolecular Cl<sup>-</sup> channels presented apoptosis-inducing activity. Matile et al have used transport of ions through ion channels as a tool to explore weak non-covalent interactions, such as anion-π interactions, halogen bonds and anion macrodipole interactions etc.

Synthetic channels with specific membrane-insertion selectivity in the bacteria membrane over that of mammalian cells usually exhibit efficient antimicrobial activity.<sup>[111]</sup> So far related reports are limited, and mostly are peptide-incorporated architecture designs. Several groups have well contributed their work in this field, toward the development of active antibacterial agents.<sup>[112-116]</sup> As an example, Hou et al.<sup>[114]</sup> have presented that synthetic tubular Pillararene channels can be finely tuned to have a high antimicrobial activity and low hemolytic toxicity, resulting from high affinity towards lipid bilayer of Gram-positive bacteria over erythrocytes.

The gating behavior is another very important feature for natural channels like channelrhodopsin, etc.<sup>[14]</sup> Among ion channels fabricated via assembly strategy, gated channels has received particular interest due to their ability to turn ON/OFF ion permeability like a “switch” when they’re exposed to certain external stimuli, with promising applications in drug-controlled release, biosensing or signal transduction, etc. Generally, their structural design involve the inclusion of “smart” elements sensitive to specific signals into the channel assembly process. For instance, reported photosensitive groups including azobenzene, spiropyran, or

---

retinal<sup>[117]</sup> have been thoroughly utilized as building blocks for light-irradiated channel construction. Kobuke,<sup>[118]</sup> Matile<sup>[119]</sup> and Hou<sup>[120]</sup> reported synthetic macrodipole or charged superstructures for voltage sensors. Although reports about completely self-assembled supramolecular channel with pH-responsiveness are limited, there're already synthetic carriers available that exhibit proton-gated behavior, like pseudopeptidic cage reported by Alfonso group,<sup>[121]</sup> phenylthiosemicarbazone<sup>[71]</sup> and thiosquaramide,<sup>[66]</sup> reported by Gale group, or bis(sulfonamide)-based carrier<sup>[58]</sup> reported by Talukdar group's. Ligand internalization is another internal stimulus to trigger ion transport through assembled channels. Examples about ligand-activated channel could be found in the work by Matile,<sup>[122]</sup> Webb<sup>[123]</sup> and Kinbara<sup>[124]</sup> groups involving the improvement from irreversible to reversible control over ion conduction. Huang<sup>[125]</sup> and Li<sup>[126]</sup>, et al. recently exploited host-guest interaction as temperature trigger during the building of thermosensitive channel, which turned out to be a successful strategy. There are also, important challenges facing this field. It is still difficult to predict a rational design for the construction of functional self-assembled ion channels. They are large architectures which can dynamically decompose or recombine within the membrane. Precise synthetic strategies for preparing large functional translocating systems are not yet available and their structures are mostly unknown. The examination of highly promising channels is important for a predictable and reliable description of the exact superstructure that can generate the single-channel currents. Single-channel currents can report on overall dimensional behaviors of the channels, but not on how the chemical binding or ion diffusion takes place within the channel at the supramolecular level. Pioneering work on the implementation of known single crystal structures and packing or theoretical modelled structures are available.



---

However, they are representing only represent partial snapshot images of the overall knowledge of their dynamics within bilayer membranes.<sup>[110]</sup>

So far, the precise design of complex supramolecular systems is still in infancy and combinatorial strategies using libraries of active simple molecules remain as promising important challenge for the future. The construction of highly performant of channels can be obtained through the combinatorial selection via synergetic combination of components. Compared with classical design of the channels in which the momomers once added one by one in a controlled manner to the backbone they cannot be exchanged *via* reversible processes, a dynamic combinatorial channel may change their constitution *via* reversible exchanges of monomeric constituents. This is giving rise to new dynamic constitutional entities presenting modulation of their structure in response to internal membrane structural constraints or to external stimuli or experimental factors

Overall scientific impact that artificial supramolecular channels provides, is related to knowledge including:

1. The *supramolecular construction* of the channels one critical hallmark for mimicking protein channels, or doing better. The controlled interactions of the ions/water with the channels reaching perfectly stabilized water wire will give rise to novel strategies to build up *artificial channels*.
2. The result of the *fast-biomimetic transport* might have high benefits and important practical applications like *advanced desalination*, or the *production of ultrapure water for biomedical or electronic industry use* or one-step purification of highly diluted solutions. We believe that

---

supramolecular artificial channels hold the potential to become integral part of cutting-edge technologies.

**Acknowledgements.** This work was supported by Agence Nationale de la Recherche ANR-18-CE06-0004-02, WATERCHANNELS. S.-P. Z. and L.-B. H. wishes to thank China Scholarship Council for the financial support.

### **Conflict of interest**

The authors declare no conflict of interest.

### **References**

- [1] a) N. Sakai, J. Mareda, S. Matile, *Mol. BioSyst.*, **2007**, *3*, 658–666; b) N. Sakai, S. Matile, *Langmuir* **2013**, *29*, 9031–9040; c) T. M. Fyles, *Chem. Soc. Rev.*, **2007**, *36*, 335–347; d) J. K. W. Chui, T. M. Fyles, *Chem. Soc. Rev.*, **2012**, *41*, 148–175; e) M. Barboiu, *Acc. Chem. Res.* **2018**, *51*, 2711–2718; f) M. Barboiu, *Angew. Chem.* **2012**, *124* 11842-11844; *Angew. Chem. Int. Ed.* **2012**, *51* 11674-11676; g) M. Barboiu, A. Gilles, *Acc. Chem. Res.* **2013**, *46*, 2814–2823; h) M. Barboiu, *Chem Commun.* **2016**, *52*, 5657-5665; i) B. Gong, *Faraday Discuss.* **2018**, *209*, 415-427; j) I. Kocsis, Z. Sun, Y. M. Legrand, M. Barboiu, *npj Clean Water* **2018**, *1*, 13; k) W. Song, M. Kumar, *Curr. Op. Chem. Eng.* **2019**, *25*, 9-17.
- [2] a) J. K. Chui, T. M. Fyles, *Org. Biomol. Chem.* **2014**, *12*, 3622-3634; b) Y. El Ghoul, R. Renia, I. Faye, S. Rassou, N. Badi, V. Bennevault-Celton, C. Huin, P. Guegan, *Chem. Commun.* **2013**, *49*, 11647-11649.
- [3] Z. Sun, M. Barboiu, *Front. Chem.* **2019**, *7*, 611.

- 
- [4] a) K. S. Iqbal, P. J. Cragg, *Dalton Trans.* **2007**, 26-32; b) D. T. Schühle, J. A. Peters, J. Schatz, *Coord. Chem. Rev.* **2011**, 255, 2727-2745; c) S. B. Nimse, T. Kim, *Chem. Soc. Rev.* **2013**, 42, 366-386.
- [5] a) W.-X. Feng, Z. Sun, M. Barboiu, *Israel J. Chem* **2018**; b) W. Si, P. Xin, Z. T. Li, J. L. Hou, *Acc. Chem. Res.* **2015**, 48, 1612-1619.
- [6] a) G. W. Gokel, *Chem. Commun.* **2000**, 1-9; b) G. W. Gokel, A. Mukhopadhyay, *Chem. Soc. Rev.* **2001**, 30, 274-286; c) G. W. Gokel, S. Negin, *Acc. Chem. Res.* **2013**, 46, 2824-2833; d) S. Negin, B. A. Smith, A. Unger, W. M. Leevy, G. W. Gokel, **2013**, 2013, 1-11; e) M. B. Patel, A. Stavri, N. S. Curvey, G. W. Gokel, *Chem. Commun.* **2014**, 50, 11562; f) S. Negin, M. B. Patel, M. R. Gokel, J. W. Meisel, G. W. Gokel, *ChemBioChem.* **2016**, 17, 2153-2161; g) S. Negin, B. A. Smith, A. Unger, W. M. Leevy and G. W. Gokel, *Int. J. Biomed. Imag.*, **2013**, 2013, 11.
- [7] T. M. Fyles, *Acc. Chem. Res.* **2013**, 46, 2847-2855.
- [8] F. Otis, M. Auger, N. Voyer, *Acc. Chem. Res.* **2013**, 46, 2934-2943.
- [9] a) A. Cazacu, C. Tong, A. van der Lee, T. M. Fyles, M. Barboiu, *J. Am. Chem. Soc.*, **2006**, 128, 9541-9548; b) M. Barboiu, *J. Incl. Phenom. Macrocycl. Chem.* **2004**, 49, 133-137; c) A. Gilles, M. Barboiu, *J. Am. Chem. Soc.* **2016**, 138, 426-432.
- [10] Y. H. Li, S. Zheng, Y. M. Legrand, A. Gilles, A. Van der Lee, M. Barboiu, *Angew. Chem.* **2018**, 130, 10680-10684; *Angew. Chem. Int. Ed.* **2018**, 57, 10520-10524.
- [11] a) Z. Sun, M. Barboiu, Y. M. Legrand, E. Petit, A. Rotaru, *Angew. Chem.* **2015**, 127, 14681-14685; *Angew. Chem. Int. Ed.* **2015**, 54, 14473-14477 b) Z. Sun, A. Gilles, I. Kocsis, Y. M. Legrand, E. Petit, M. Barboiu, *Chem. Eur. J.* **2016**, 22, 2158-2164;

- 
- [12] C. Ren, J. Shen, H. Zeng, *J. Am. Chem. Soc.* **2017**, *139*, 12338-12341.
- [13] S. Schneider, E. D. Licsandru, I. Kocsis, A. Gilles, F. Dumitru, E. Moulin, J. Tan, J. M. Lehn, N. Giuseppone, M. Barboiu, *J. Am. Chem. Soc.* **2017**, *139*, 3721-3727.
- [14] J.-Y. Chen, J.-L. Hou, *Org. Chem. Front.* **2018**, *5*, 1728-1736.
- [15] a) R.-Y. Yang, C.-Y. Bao, Q.-N. Lin, L.-Y. Zhu, *Chin. Chem. Lett.* **2015**, *26*, 851-856; b) T. Liu, C. Bao, H. Wang, L. Fei, R. Yang, Y. Long, L. Zhu, *New J. Chem.* **2014**, *38*, 3507-3513; c) C. Bao, M. Ma, F. Meng, Q. Lin, L. Zhu, *New J. Chem.* **2015**, *39*, 6297-6302; d) T. Liu, C. Bao, H. Wang, Y. Lin, H. Jia, L. Zhu, *Chem. Commun.* **2013**, *49*, 10311-10313; e) P. V. Jog, M. S. Gin, *Org. Lett.* **2008**, *10*, 3693-3696; f) Y. Sueishi, M. Kasahara, M. Inoue, K. Matsueda, *J. Incl. Phenom. Macro.* **2003**, *46*, 71-75; g) P. V. P, T. Scheuer, W. A. Catterall, *Proc. Natl. Acad. Sci.* **1989**, *86*, 8147-8151.
- [16] Y. Zhou, Y. Chen, P. P. Zhu, W. Si, J. L. Hou, Y. Liu, *Chem. Commun.* **2017**, *53*, 3681-3684.
- [17] S. Chen, Y. Wang, T. Nie, C. Bao, C. Wang, T. Xu, Q. Lin, D.-H. Qu, X. Gong, Y. Yang, L. Zhu, H. Tian, *J. Am. Chem. Soc.* **2018**, *140*, *51*, 17992 – 17998.
- [18] R. Ye, C. Ren, J. Shen, N. Li, F. Chen, A. Roy, H. Zeng, *J. Am. Chem. Soc.* **2019**, *141*, 9788 – 9792.
- [19] J. Montenegro, M. R. Ghadiri, J. R. Granja, *Acc. Chem. Res.* **2013**, *46*, 2955-2965.
- [20] a) M. R. Ghadiri, J. R. Granja, L. K. Buehler, *Nature* **1994**, *369*, 301-304; b) T. D. Clark, L. K. Buehler, M. R. Ghadiri, *J. Am. Chem. Soc.* **1998**, *120*, 651-656; c) K. Motesharei, M. R. Ghadiri, *J. Am. Chem. Soc.* **1997**, *119*, 11306-11312.

- 
- [21] a) J. R. Granja, M. R. Ghadiri, *J. Am. Chem. Soc.* **1994**, *116*, 10785-10786; b) J. Sánchez-Quesada, H. Sun Kim, M. R. Ghadiri, *Angew. Chem.* **2001**, *113*, 2571-2574; *Angew. Chem. Int. Ed.* **2001**, *40*, 2503-2506.
- [22] B. Gong, Z. Shao, *Acc. Chem. Res.* **2013**, *46*, 2856-2866.
- [23] A. J. Hessel, A. L. Brown, K. Yamato, W. Feng, L. Yuan, A. J. Clements, S. V. Harding, G. Szabo, Z. Shao, B. Gong, *J. Am. Chem. Soc.* **2008**, *130*, 15784-15785.
- [24] M. A. Kline, X. Wei, I. J. Horner, R. Liu, S. Chen, K. Y. Yung, K. Yamato, Z. Cai, F. V. Bright, X. C. Zeng, B. Gong, *Chem. Sci.* **2015**, *6*, 152-157.
- [25] X. Zhou, G. Liu, K. Yamato, Y. Shen, R. Cheng, X. Wei, W. Bai, Y. Gao, H. Li, Y. Liu, F. Liu, D. M. Czajkowsky, J. Wang, M. J. Dabney, Z. Cai, J. Hu, F. V. Bright, L. He, X. C. Zeng, Z. Shao, B. Gong, *Nat. Commun.* **2012**, *3*, 949.
- [26] a) H. Mamad-Hemouch, L. Bacri, C. Huin, C. Przybylski, B. Thiebot, G. Patriarche, N. Jarroux, J. Pelta, *Nanoscale* **2018**, *10*, 15303-15316; b) L. Bacri, H. Mamad-Hemouch, C. Przybylski, B. Thiebot, G. Patriarche, N. Jarroux, J. Pelta, *Faraday Discuss.* **2018**, *210*, 41-54; c) H. Mamad-Hemouch, H. Ramoul, M. Abou Taha, L. Bacri, C. Huin, C. Przybylski, A. Oukhaled, B. Thiebot, G. Patriarche, N. Jarroux, J. Pelta, *Nano Lett.* **2015**, *15*, 7748-7754.
- [27] Y. Jiang, A. Lee, J. Chen, M. Cadene, B. T. Chait, R. MacKinnon, *Nature* **2002**, *417*, 523-526.
- [28] P. Xin, P. Zhu, P. Su, J.-L. Hou, Z.-T. Li, *J. Am. Chem. Soc.* **2014**, *136*, 13078-13081
- [29] a) C. Lang, W. Li, Z. Dong, X. Zhang, F. Yang, B. Yang, X. Deng, C. Zhang, J. Xu, J. Liu, *Angew. Chem.* **2016**, *128*, 9875-9879; *Angew. Chem. Int. Ed.* **2016**, *55*, 9723-9727; b) C. Lang,

---

X. Deng, F. Yang, B. Yang, W. Wang, S. Qi, X. Zhang, C. Zhang, Z. Dong, J. Liu, *Angew. Chem.* **2017**, *129*, 12842-12845; *Angew. Chem. Int. Ed.* **2017**, *56*, 12668-12671.

[30] a) J. T. Davis, *Angew. Chem.* **2004**, *116*, 684-716; *Angew. Chem. Int. Ed.* **2004**, *43*, 668-698; b) J. T. Davis, G.P. Spada, *Chem Soc. Rev.* **2007**, *36*, 296-313; c) C. Arnal-Herault, M. Michau, A. Pasc-Banu, M. Barboiu, *Angew. Chem.* **2007**, *119*, 4346-4350; *Angew. Chem. Int. Ed.*, 2007, **46**, 4268-4272; d) C. Arnal-Herault, A. Pasc-Banu, M. Michau, D. Cot, E. Petit, M. Barboiu, *Angew. Chem.* **2007**, *119*, 8561-8565; *Angew. Chem. Int. Ed.*, 2007, **46**, 8409-8413; e) S. Mihai, Y. Le Duc, D. Cot, M. Barboiu, *J. Mater Chem*, **2010**, *20*, 9443-9448.

[31] C. Li, N. Sakai, S. T. Moshiri, S. Matile, *Tetrahedron Lett.* **1998**, *39*, 3627-3630.

[32] a) S. L. Forman, J. C. Fettinger, S. Pieraccini, G. Gottarelli, J. T. Davis, *J. Am. Chem. Soc.* **2000**, *122*, 4060-4067; b) M. S. Kaucher, W. A. Harrell, J. T. Davis, *J. Am. Chem. Soc.* **2006**, *128*, 38 – 39.

[33] R. N. Das, Y. P. Kumar, S. A. Kumar, O. M. Schütte, C. Steinem, J. Dash, *Chem. Eur. J.* **2018**, *24*, 4002 – 4005.

[34] N. Sakai, Y. Kamikawa, M. Nishii, T. Matsuoka, T. Kato, S. Matile, *J. Am. Chem. Soc.* **2006**, *128*, 2218-2219.

[35] R. N. Das, Y. P. Kumar, O. M. Schutte, C. Steinem, J. Dash, *J. Am. Chem. Soc.* **2015**, *137*, 34-37.

[36] a) I. Tabushi, Y. Kuroda, K. Yokota, *Tetrahedron Lett.* **1982**, *23*, 4601-4604; b) A. J. M. V. Beijnen, R. J. M. Nolte, J. W. Zwikker, W. Drenth, *Recl. Trav. Chim. Pay-Bas* **1982**, *101*, 409-410.

[37] H. Furukawa, K. E. Cordova, M. O'Keeffe, O. M. Yaghi, *Science* **2013**, *341*, 1230444.

- 
- [38] a) T. M. Fyles, C. C. Tong, *New J. Chem.* **2007**, *31*, 655-661; b) M. Fujita, J. Yazaki, K. Ogura, *J. Am. Chem. Soc.*, **1990**, *12*, 5645–5647.
- [39] H. Furukawa, J. Kim, K. E. Plass, O. M. Yaghi, *J. Am. Chem. Soc.* **2006**, *128*, 8398-8399.
- [40] M. Jung, H. Kim, K. Baek, K. Kim, *Angew. Chem.* **2008**, *120*, 5839-5841; *Angew. Chem. Int. Ed.* **2008**, *47*, 5755-5757.
- [41] R. Kawano, N. Horike, Y. Hijikata, M. Kondo, A. Carné-Sánchez, P. Larpent, S. Ikemura, T. Osaki, K. Kamiya, S. Kitagawa, S. Takeuchi, S. Furukawa, *Chem* **2017**, *2*, 393-403.
- [42] a) A. Müller, S. K. Das, E. Krickemeyer, C. Kuhlmann, *Inorg. Synth.*, **2004**, *34*, 191-200; b) A. Müller, E. Krickemeyer, H. Bögge, M. Schmidtman, F. Peters, *Angew. Chem.* **1998**, *110*, 3567-3571; *Angew. Chem. Int. Ed.* **1998**, *37*, 3360-3363.
- [43] A. Müller, Y. Zhou, H. Bögge, M. Schmidtman, T. Mitra, E. T. K. Haupt, A. Berkle, *Angew. Chem.* **2006**, *118*, 474-479; *Angew. Chem. Int. Ed.* **2006**, *45*, 460-465.
- [44] E. Mahon, S. Garai, A. Müller, M. Barboiu, *Adv. Mater.* **2015**, *27*, 5165-5170.
- [45] a) S. Negin, M. M. Daschbach, O. V. Kulikov, N. Rath, G. W. Gokel, *J Am Chem Soc* **2011**, *133*, 3234-3237; b) R. Li, O. V. Kulikov, G. W. Gokel, *Chem. Commun.* **2009**, 6092-6094. c) O. V. Kulikov, M. M. Daschbach, C. R. Yamnitz, N. Rath, G. W. Gokel, *Chem. Commun.* **2009**, 7497-7499.
- [46] O. V. Kulikov, R. Li, G. W. Gokel, *Angew. Chem.* **2009**, *121*, 381-383; *Angew. Chem. Int. Ed.* **2009**, *48*, 375-377.
- [47] a) A. Vidyasagar, K. Handore, K. M. Sureshan, *Angew. Chem.* **2011**, *123*, 8171-8174; *Angew. Chem. Int. Ed.* **2011**, *50*, 8021-8024; b) T. Saha, S. Dasari, D. Tewari, A. Prathap, K.



---

M. Sureshan, A. K. Bera, A. Mukherjee, P. Talukdar, *J. Am. Chem. Soc.* **2014**, *136*, 14128-14135.

[48] a) N. Busschaert, P. A. Gale, *Angew. Chem.* **2013**, *125*, 1414–1422; *Angew. Chem. Int. Ed.* **2013**, *52*, 1374–1382; b) N. Busschaert, C. Caltagirone, W. V. Rossom, P. A. Gale, *Chem. Rev.* **2015**, *115*, 15, 8038-8155.

[49] a) K. W. C. Jonathan, T. M. Fyles, *Org. Biomol. Chem.* **2014**, *12*, 3622-3634; b) T. Saha, A. Roy, M. L. Gening, D. V. Titov, A. G. Gerbst, Y. E. Tsvetkov, N. E. Nifantiev, P. Talukdar, *Chem. Commun.* **2014**, *50*, 5514-5516.

[50] S. N. Berry, V. Soto-Cerrato, E. N. W. Howe, H. J. Clarke, I. Mistry, A. Tavassoli, Y. T. Chang, R. Perez-Tomas, P. A. Gale, *Chem. Sci.* **2016**, *7*, 5069-5077.

[51] H. Valkenier, C. J. E. Haynes, J. Herniman, P. A. Gale, A. P. Davis, *Chem. Sci.* **2014**, 1128-1134.

[52] C. M. Dias, H. Li, H. Valkenier, L. E. Karagiannidis, P. A. Gale, D. N. Sheppard, A. P. Davis, *Org. Biomol. Chem.* **2018**, *16*, 1083-1087.

[53] A. Roy, D. Saha, A. Mukherjee, P. Talukdar, *Org. Lett.* **2016**, *18*, 5864-5867.

[54] X. Wu, P. A. Gale, *J. Am. Chem. Soc.* **2016**, *138*, 16508-16514.

[55] M. J. Spooner, H. Li, I. Marques, P. M. R. Costa, X. Wu, E. N. W. Howe, N. Busschaert, S. J. Moore, M. E. Light, D. N. Sheppard, V. Felix, P. A. Gale, *Chem. Sci.* **2019**, *10*, 1976-1985.

[56] N. Busschaert, M. Wenzel, M. E. Light, P. Iglesias-Hernandez, R. Perez-Tomas, P. A. Gale, *J. Am. Chem. Soc.* **2011**, *133*, 14136-14148.

[57] T. Saha, M. S. Hossain, D. Saha, M. Lahiri, P. Talukdar, *J. Am. Chem. Soc.* **2016**, *138*, 7558-7567.

- 
- [58] A. Roy, O. Biswas, P. Talukdar, *Chem. Commun.* **2017**, *53*, 3122-3125.
- [59] C. R. Yamnitz, S. Negin, I. A. Carasel, R. K. Winter, G. W. Gokel, *Chem. Commun.* **2010**, *46*, 2838-2840.
- [60] J. T. Davis, P. A. Gale, O. A. Okunola, P. Prados, J. C. Iglesias-Sanchez, T. Torroba, R. Quesada, *Nature Chem.* **2009**, *1*, 138-144.
- [61] P. A. Gale, J. Garric, M. E. Light, B. A. McNally, B. D. Smith, *Chem. Commun.* **2007**, 1736-1738.
- [62] N. Busschaert, I. L. Kirby, S. Young, S. J. Coles, P. N. Horton, M. E. Light, P. A. Gale, *Angew. Chem.* **2012**, *124*, 4502-4506; *Angew. Chem. Int. Ed.* **2012**, *51*, 4426-4430.
- [63] S. J. Edwards, H. Valkenier, N. Busschaert, P. A. Gale, A. P. Davis, *Angew. Chem.* **2015**, *127*, 4675-4679; *Angew. Chem. Int. Ed.* **2015**, *54*, 4592-4596.
- [64] N. Busschaert, S. H. Park, K. H. Baek, Y. P. Choi, J. Park, E. N. W. Howe, J. R. Hiscock, L. E. Karagiannidis, I. Marques, V. Felix, W. Namkung, J. L. Sessler, P. A. Gale, I. Shin, *Nature Chem.* **2017**, *9*, 667-675.
- [65] X. Wu, N. Busschaert, N. J. Wells, Y. B. Jiang, P. A. Gale, *J Am Chem Soc* **2015**, *137*, 1476-1484.
- [66] N. Busschaert, R. B. Elmes, D. D. Czech, X. Wu, I. L. Kirby, E. M. Peck, K. D. Hendzel, S. K. Shaw, B. Chan, B. D. Smith, K. A. Jolliffe, P. A. Gale, *Chem. Sci.* **2014**, *5*, 3617-3626.
- [67] R. B. Elmes, N. Busschaert, D. D. Czech, P. A. Gale, K. A. Jolliffe, *Chem. Commun.* **2015**, *51*, 10107-10110.
- [68] S. J. Moore, M. Wenzel, M. E. Light, R. Morley, S. J. Bradberry, P. Gómez-Iglesias, V. Soto-Cerrato, R. Pérez-Tomás, P. A. Gale, *Chem. Sci.* **2012**, *3*, 2501-2509.

- 
- [69] G. W. Bates, P. A. Gale, M. E. Light, *Chem. Commun.* **2007**, 2121-2123.
- [70] L. A. Jowett, E. N. W. Howe, V. Soto-Cerrato, W. Van Rossom, R. Perez-Tomas, P. A. Gale, *Sci. Rep.* **2017**, *7*, 9397.
- [71] E. N. Howe, N. Busschaert, X. Wu, S. N. Berry, J. Ho, M. E. Light, D. D. Czech, H. A. Klein, J. A. Kitchen, P. A. Gale, *J. Am. Chem. Soc.* **2016**, *138*, 8301-8308.
- [72] P. I. Hernandez, D. Moreno, A. A. Javier, T. Torroba, R. Perez-Tomas, R. Quesada, *Chem. Commun.* **2012**, 1556-1558.
- [73] N. J. Knight, E. Hernando, C. J. E. Haynes, N. Busschaert, H. J. Clarke, K. Takimoto, M. Garcia-Valverde, J. G. Frey, R. Quesada, P. A. Gale, *Chem. Sci.* **2016**, *7*, 1600-1608.
- [74] A. Roy, D. Saha, P. S. Mandal, A. Mukherjee, P. Talukdar, *Chem. Eur J.* **2017**, *23*, 1241-1247.
- [75] S. V. Shinde, P. Talukdar, *Angew. Chem.* **2017**, *129*, 4302-4306; *Angew. Chem. Int. Ed.* **2017**, *56*, 4238-4242.
- [76] H. J. Clarke, E. N. Howe, X. Wu, F. Sommer, M. Yano, M. E. Light, S. Kubik, P. A. Gale, *J. Am. Chem. Soc.* **2016**, *138*, 16515-16522.
- [77] C. R. Bondy, P. A. Gale, S. J. Loeb, *J. Am. Chem. Soc.* **2004**, *126*, 5030-5031.
- [78] C. Caltagirone, A. Mulas, F. Isaia, V. Lippolis, P. A. Gale, M. E. Light, *Chem. Commun.* **2009**, 6279-6281.
- [79] a) N. R. Williamson, P. C. Fineran, F. J. Leeper, G. P. C. Salmond, *Nat. Rev. Microbiol.* **2006**, 887-899; b) S. Ohkuma, T. Sato, M. Okamoto, H. Matsuya, K. Arai, T. Kataoka, K. Nagai, H. H. Wasserman, *Biochem. J.* **1998**, 731-741.
- [80] C. A. Lipinski, F. Lombardo, B. W. Dominy, P. J. Feeney, *Adv. Drug Delivery Rev.* **1997**,

---

23, 3-25.

[81] S. Matile, N. Sakai, A. Hennig, *Supramolecular chemistry : From Molecules to Nanomaterials* **2012**.

[82] T. Saha, A. Gautam, A. Mukherjee, M. Lahiri, P. Talukdar, *J. Am. Chem. Soc.* **2016**, *138*, 16443-16451.

[83] A. Roy, A. Gautam, J. A. Malla, S. Sarkar, A. Mukherjee, P. Talukdar, *Chem. Commun.* **2018**, *54*, 2024-2027.

[84] a) P. H. Schlesinger, R. Ferdani, J. Liu, J. Pajewska, R. Pajewski, M. Saito, H. Shabany, G. W. Gokel, *J. Am. Chem. Soc.* **2002**, *124*, 1848-1849; b) L. You, R. Li, G. W. Gokel, *Org. Biomol. Chem.* **2008**, *6*, 2914-2923; c) L. You, R. Ferdani, G. W. Gokel, *Chem. Commun.* **2006**, 603-605.

[85] G. A. Cook, R. Pajewski, M. Aburi, P. E. Smith, O. Prakash, J. M. Tomich, G. W. Gokel, *J. Am. Chem. Soc.* **2006**, *128*, 1633-1638.

[86] S. S. Burade, S. V. Shinde, N. Bhuma, N. Kumbhar, A. Kotmale, P. R. Rajamohanan, R. G. Gonnade, P. Talukdar, D. D. Dhavale, *J. Org. Chem.* **2017**, *82*, 5826-5834.

[87] C. Ren, F. Zeng, J. Shen, F. Chen, A. Roy, S. Zhou, H. Ren, H. Zeng, *J. Am. Chem. Soc.* **2018**, *140*, 8817-8826.

[88] F. Zeng, F. Liu, L. Yuan, S. Zhou, J. Shen, N. Li, H. Ren, H. Zeng, *Org. Lett.* **2019**, *21*, 4826-4830.

[89] X. Li, B. Shen, X.-Q. Yao, D. Yang, *J. Am. Chem. Soc.* **2007**, *129*, 7264-7265.

[90] X. Li, B. Shen, X. Q. Yao, D. Yang, *J. Am. Chem. Soc.* **2009**, *131*, 13676-13680.

[91] B. Shen, X. Li, F. Wang, X. Yao, D. Yang, *PLoS One* **2012**, *7*, e34694.

- 
- [92] L. C. Gilday, S. W. Robinson, T. A. Barendt, M. J. Langton, B. R. Mullaney, P. D. Beer, *Chem. Rev.* **2005**, *115*, 7118-7195.
- [93] a) A. V. Jentzsch, D. Emery, J. Mareda, P. Metrangolo, G. Resnati, S. Matile, *Angew. Chem.* **2011**, *123*, 11879-11882; *Angew. Chem. Int. Ed.* **2011**, *50*, 11675-11678; b) A. V. Jentzsch, D. Emery, J. Mareda, S. K. Nayak, P. Metrangolo, G. Resnati, N. Sakai, S. Matile, *Nat. Commun.* **2012**, *3*, 905.
- [94] L. M. Lee, M. Tsemperouli, A.I. Poblador-Bahamonde, S. Benz, N. Sakai, K. Sugihara, S. Matile, *J. Am. Chem. Soc.* **2019**, *141*, 810–814.
- [95] A. V. Jentzsch, S. Matile, *J. Am. Chem. Soc.* **2013**, *135*, 5302-5303.
- [96] C. Ren, X. Ding, A. Roy, J. Shen, S. Zhou, F. Chen, S. F. Yau Li, H. Ren, Y. Y. Yang, H. Zeng, *Chem. Sci.* **2018**, *9*, 4044-4051.
- [97] V. Gorteau, G. Bollot, J. Mareda, A. Perez-Velasco, S. Matile, *J. Am. Chem. Soc.* **2006**, *128*, 14788 – 14789.
- [98] V. Gorteau, G. Bollot, J. Mareda, S. Matile, *Org. Biomol. Chem.* **2007**, *5*, 3000 –3012.
- [99] V. Gorteau, M. D. Julliard, S. Matile, *J. Membr. Sci.* **2008**, *321*, 37– 42.
- [100] A. Perez-Velasco, V. Gorteau, S. Matile, *Angew. Chem.* **2008**, *120*, 935 – 937; *Angew. Chem. Int. Ed.* **2008**, *47*, 921 –923.
- [101] J. Mareda, S. Matile, *Chem. Eur. J.* **2009**, *15*, 28 – 37.
- [102] D. Quiçonero, C. Garau, C. Rotger, A. Frontera, P. Ballester, A. Costa, P. M. Deya, *Angew. Chem.* **2002**, *114*, 3539 – 3542; *Angew. Chem. Int. Ed.* **2002**, *41*, 3389 – 3392.
- [103] M. Mascal, I. Yakovlev, E. B. Nikitin, J. C. Fettinger, *Angew. Chem.* **2007**, *119*, 8938 – 8940; *Angew. Chem. Int. Ed.* **2007**, *46*, 8782 –8784.

- 
- [104] D.-X. Wang, M.-X. Wang, *J. Am. Chem. Soc.* **2013**, *135*, 892–897.
- [105] O. B. Berryman, V. S. Bryantsev, D. P. Stay, D. W. Johnson, B. P. Hay, *J. Am. Chem. Soc.* **2007**, *129*, 48-58.
- [106] S. P. Zheng, Y. H. Li, J. J. Jiang, A. van der Lee, D. Dumitrescu, M. Barboiu, *Angew. Chem.* **2019**, *131*, 12165–12170; *Angew. Chem. Int. Ed.* **2019**, *58*, 12037-12042.
- [107] B. P. Benke, P. Aich, Y. Kim, K. L. Kim, M. R. Rohman, S. Hong, I. C. Hwang, E. H. Lee, J. H. Roh, K. Kim, *J Am Chem Soc* **2017**, *139*, 7432-7435.
- [108] a) C. J. E. Haynes, J. Zhu, C. Chimerele, S. Hernandez-Ainsa, I. A. Riddell, T. K. Ronson, U. F. Keyser, J. R. Nitschke, *Angew. Chem. Int. Ed.* **2017**, *56*, 15388-15392; b) I. A. Riddell, Y. R. Hristova, J. K. Clegg, C. S. Wood, B. Breiner, J. R. Nitschke, *J. Am. Chem. Soc.* **2013**, *135*, 2723-2733.
- [109] L. Tapia, Y. Pérez, M. Bolte, J. Casas, J. Solà, R. Quesada, I. Alfonso, *Angew. Chem.* **2019**, *131*, 12595–12598; *Angew. Chem. Int. Ed.*, **2019**, *58*, 12465-12468.
- [110] E. Licsandru, I. Kocsis, Y.-x. Shen, S. Murail, Y.-M. Legrand, A. van der Lee, D. Tsai, M. Baaden, M. Kumar, M. Barboiu, *J. Am. Chem. Soc.*, **2016**, *138*, 5403-5409.
- [111] J. Pogliano, N. Pogliano, J. A. Silverman, *J. Bacteriol.*, **2012**, *194*, 4494 - 4504.
- [112] S. Fernandez-Lopez, H. - S. Kim, E. C. Choi, M. Delgado, J. R. Granja, *Nature*, **2001**, *412*, 452 - 455.
- [113] a) W. M. Leevy, G. M. Donato, R. Ferdani, W. E. Goldman, P. H. Schlesinger, G. W. Gokel, *J. Am. Chem. Soc.*, **2002**, *124*, 9022 - 9023; b) J. W. Meisel, M. B. Patel, E. Garrad, R. A. Stanton, G. W. Gokel, *J. Am. Chem. Soc.*, **2016**, *138*, 10571 - 10577.

- 
- [114] a) M. Zhang, P.-P. Zhu, P. Xin, W. Si, Z.-T. Li, and J.-L. Hou, *Angew. Chem. Int. Ed.*, **2017**, 56, 2999 - 3003. b) W.-W. Haoyang, M. Zhang and J.-L. Hou, *Chin. J. Chem.*, **2019**, 37, 25 - 29.
- [115] J. Mao, T. Kuranaga, H. Hamamoto, K. Sekimizu and M. Inoue, *Chem. Med. Chem.*, **2015**, 10, 540 - 545.
- [116] D. N. Reddy, S. Singh, C. M. W. Ho, J. Patel, P. Schlesinger, S. Rodgers, A. Doctor and G. R. Marshall, *Eur. J. Med. Chem.*, **2018**, 149, 193 - 210.
- [117] M. R. Banghart, M. Volgraf and D. Trauner, *Biochemistry*, **2006**, 45, 15129-15141.
- [118] a) C. Goto, M. Yamamura, A. Satake and Y. Kobuke, *J. Am. Chem. Soc.*, **2001**, 123, 12152-12159. b) Y. Kobuke and T. Nagatani, *J. Org. Chem.*, **2001**, 66, 5094.
- [119] J.-Y. Winum and S. Matile, *J. Am. Chem. Soc.* **1999**, 121, 7961-7962.
- [120] W. Si, Z.-T. Li, and J.-L. Hou, *Angew. Chem. Int. Ed.*, **2014**, 53, 4578-4581.
- [121] L. Tapia, Y. Pérez, M. Bolte, J. Casas, J. Solà, R. Quesada and I. Alfonso, *Angew. Chem. Int. Ed.*, **2019**, 131(36), 12595-12598.
- [122] a) V. Gorteau, F. Perret, G. Bollot, J. Mareda, A. N. Lazar, A. W. Coleman, D.- H. Tran, N. Sakai and S. Matile, *J. Am. Chem. Soc.*, **2004**, 126, 13592-13593. b) P. Talukdar, G. Bollot, J. Mareda, N. Sakai and S. Matile, *J. Am. Chem. Soc.*, **2005**, 127, 6528-6529; c) S. Bhosale, A. L. Sisson, P. Talukdar, A. Fürstenberg, N. Banerji, E. Vauthey, G. Bollot, J. Mareda, C. Röger, F. Wurthner, N. Sakai and S. Matile, *Science*, **2006**, 313, 84-86; d) P. Talukdar, G. Bollot, J. Mareda, N. Sakai and S. Matile, *Chem.-Eur. J.*, **2005**, 11, 6525-6532.
- [123] a) C. P. Wilson and S. J. Webb, *Chem. Commun.*, **2008**, 4007-4009; b) C. P. Wilson, C. Boglio, L. Ma, S. L. Cockroft and S. J. Webb, *Chem.-Eur. J.*, **2011**, 17, 3465-3473.

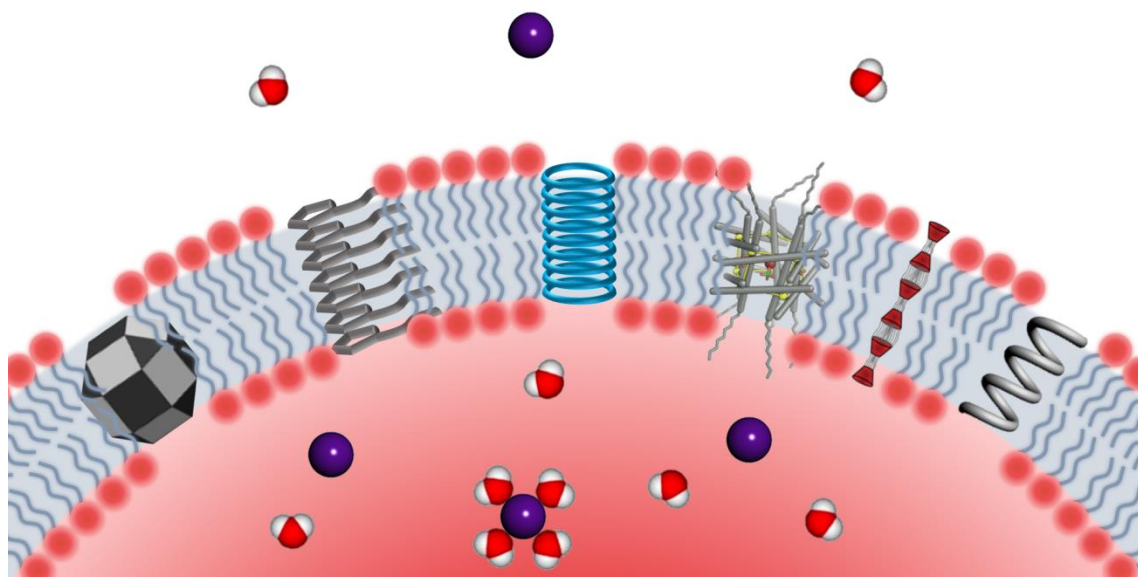


[124] T. Muraoka, T. Endo, K. V. Tabata, H. Noji, S. Nagatoishi, K. Tsumoto, R. Li and K. Kinbara, *J. Am. Chem. Soc.*, **2014**, *136*, 15584-15595.

[125] S. Y. Dong, B. Zheng, Y. Yao, C. Y. Han, J. Y. Yuan, M. Antonietti and F. H. Huang, *Adv. Mater.*, **2013**, *25*, 6864.

[126] a) J. Bi, X. Zeng, D. Tian and H. Li, *Org. Lett.*, **2016**, *18*, 1092-1095. b) R. Wang, Y. Sun, F. Zhang, M. Song, D. Tian and H. Li, *Angew. Chem. Int. Ed.*, **2017**, *56*, 5294-5298.

---

**Table of contents**

**TOC text:** Schematic overview of the various types of supramolecular Self-assembled Artificial Ion-Channels: capsules and cages, macrocyclic stacks, tubular helical architectures.